REPUBLIC OF TURKEY
ACIBADEM MEHMET ALİ AYDINLAR UNIVERSITY
INSTITUTE OF HEALTH SCIENCES

SELECTIVE INHIBITION OF MLH1 DEFICIENT COLON CANCER GROWTH BY NOVEL DNA POLYMERASE GAMMA INHIBITOR

BERNA SOMUNCU

DOCTORATE THESIS

DEPARTMENT OF MEDICAL BIOTECHNOLOGY

SUPERVISOR
Prof. Dr. Meltem MÜFTÜOĞLU

ISTANBUL-2022

REPUBLIC OF TURKEY
ACIBADEM MEHMET ALİ AYDINLAR UNIVERSITY
INSTITUTE OF HEALTH SCIENCES

SELECTIVE INHIBITION OF MLH1 DEFICIENT COLON CANCER GROWTH BY NOVEL DNA POLYMERASE GAMMA INHIBITOR

BERNA SOMUNCU

DOCTORATE THESIS

DEPARTMENT OF MEDICAL BIOTECHNOLOGY

SUPERVISOR
Prof. Dr. Meltem MÜFTÜOĞLU

ISTANBUL-2022

Department:	Institute of Health Sciences
Program:	Medical Biotechnology
Thesis title:	Selective Inhibition Of Mlh1 Deficient Colon Cancer Growth By Novel DNA Polymerase Gamma Inhibitor
Students' name and surname:	Berna Somuncu
Date of defence:	21 / 07 / 2022

This is to certify that I have examined this copy of master thesis. I have found that she prepared after fulfilling requirements specified in the associated legislations before the final examining committee whose signatures are below.

Jury Member (Head of the Defense)	Prof. Dr. Batu Erman Bogazici University
Jury Member (Thesis Supervisor)	Prof. Dr. Meltem Müftüoğlu Acıbadem Mehmet Ali Aydınlar University
Jury member	Assoc. Prof. Emel Timuçin Acıbadem Mehmet Ali Aydınlar University
Jury member	Assoc. Prof. Meryem Sedef Erdal Istanbul University
Jury member	Assoc. Prof. Günseli Bayram Akçapınar Acıbadem Mehmet Ali Aydınlar University

DECLARATION

I declare that this thesis work is my own work, I had no unethical behavior at any stages from the planning to the writing of the thesis, I obtained all the information in this thesis in accordance with academic and ethical rules, I cited all the information and comments that were not obtained with this thesis work, and I provided resources in the list of references. I also declare that there was no violation of any patents and copyrights during the study and writing of this thesis.

21.07.2022
Berna SOMUNCU

PREFACE AND ACKNOWLEDGEMENT

I would like to express my heartfelt gratitude and thanks to Professor Meltem Müftüoğlu for making every aspect of this study possible, as well as for her invaluable scientific support and mentorship. I also would like to thank for generously providing technically exquisite environment possible and putting her trust in me.

I greatly acknowledge Professor Whitney Yin from University of Texas for the purified recombinant DNA polymerase gamma protein, Professor Aykut Üren from Georgetown University for screening small molecules, and Dr. Anatoly Zhitkovich from Brown University for providing HCT116VA/V1 cell lines. Furthermore, I am very thankful to Acıbadem Mehmet Ali Aydınlar University - DEHAM for providing us the world standard animal laboratory. I would also like to thank my Müftüoğlu group labmates, Tuğçe Ertüzün and Ayşegül Ekmekçioğlu for their help and support during this study.

Additionally, I feel very lucky to have precious my friends, Elif Tıkır, Meltem Pak, Gülnihal Bozdağ and Tuğçe Doğruel and I would like to thank for giving me infinite morale, support and love.

I wish to thank to my beloved mother, Yeter Somuncu, my dear father Hilmi Somuncu and my sincere brothers Burak, Barış and dear their wives for their support and patience during these challenging times.

This work was supported by the Scientific and Technological Research Council of Turkey (TUBITAK), grant no: 212T026 and 215S614.

TABLE OF CONTENTS

LIST OF ABBREVIATIONS

Abbreviation	Explanation
1-nt	One Nucleotide
3′-PUA	3′-phospho-α,β-unsaturated aldehydes
8-OHdG	8-hydroxydeoxyguanosine
8-oxo-G	7,8 dihydro-8-oxoguanine
AIF	Apoptosis Inducing Factor
AP	Apurinic/Apyrimidinic
APE1	Apurinic/Apyrimidinic Endonuclease
AS13	2-benzoyl-6-(2,3-dimethoxybenzylidene)-cyclohexanol
ATP	Adenosine Triphosphate
AZT-TP	3'deoxy-3'azidothymidine triphosphate
BER	Base Excision Repair
BRCA	Breast Cancer Gene
BWC	Body weight change
CR	Congo Red
CSB/CSA	Cockayne Syndrome Group B/Group A
ddN	Dideoxynucleotide
DDR	DNA Damage Response
DMEM	Dulbecco's Modified Eagle Medium: Nutrient Mixture
DNA	Deoxyribonucleic Acid
DSB	Double-strand Break
DSBR	Double-strand Break Repair
dsDNA	Double-stand DNA
ETC	Electron Transfer Chain
FBS	Fetal Bovine Serum
FDA	United States Food and Drug Administration
FEN1	Flap Structure-specific Endonuclease 1
GGR	Global Genome Repair
h	Hour
H_2O_2	Hydrogen Peroxide
HIV-1	Human Immunodeficiency Virus 1
HNPCC	Hereditary Non-polyposis Colorectal Cancer
HR	Homologous Recombination
ICL	Inter-strand Crosslinks
IDL	Insertion-deletion Loops
InPACdb	Indian plant anticancer compounds database
IR	Ionizing Radiation
KD	Dissociation Constants
LP	Long-patch

MGME1	Mitochondrial Genome Maintenance Exonuclease 1
min	Minute
MLH1	MutL homolog 1
MLH3	MutL homolog 3
MLH4	MutL homolog 4
MMR	Mismatch Repair
MPG	N-methylpurine DNA Glycosylase
MSH	MutS Homolog
mtBER	Mitochondrial Base Excision Repair
mtDNA	Mitochondrial Deoxyribonucleic Acid
mtLigIII	Mitochondrial DNA Ligase III
mtRNAP	Mitochondrial RNA Polymerase
mtSSB	Mitochondrial ssDNA Binding Protein
MUTYH	MutY Homolog
NAD^+	Nicotinamide Adenine Dinucleotide
nBER	Nuclear Base Excision Repair
nDNA	Nuclear DNA
NEIL1	Nei-like DNA Glycosylase 1
NEIL2	Nei-like DNA Glycosylase 2
NER	Nucleotide Excision Repair
NRTI	Nucleoside Reverse Transcriptase Inhibitors
NTHL1	Nth-like DNA Glycosylase 1
O_2^-	Superoxide Radical
OGG1	8-oxoguanine DNA glycosylase-1
OH	Hydroxyl Radical
PARP	Poly (ADP-ribose) Polymerase
PINK1	PTEN-induced kinase 1
PNK	Polynucleotide Kinase
PNKP	Polynucleotide Kinase/Phosphatase
Pol β	DNA polymerase β
Pol γ	DNA polymerase γ
PTEN	Phosphatase and Tensin Homolog
Rmax	Analyte Binding Capacity
RNaseH1	Ribonuclease H1
ROS	Reactive Oxygen Species
rRNA	Ribosomal Ribonucleic Acid
RTCA	Real-time cell analysis
RU	Response units
SAM	S-adenosylmethionine
siRNA	Short Interfering RNA
SP	Short-patch
SPR	Surface Plasmon Resonance
SSB	Single-strand Break

SSBR	Single-strand Break Repair
ssDNA	Single-stranded DNA
SWMD	Seaweed metabolites database
TBS-T	Tris buffer solution
TCR	Transcription-coupled Repair
TOP1	DNA Topoisomerase 1
tRNA	Transfer Ribonucleic Acid
UDG	Uracil DNA Glycosylases
XPC	Xeroderma Pigmentosum Complex
XRCC1	X-ray repair cross-complementing protein 1

LIST OF FIGURES

LIST OF TABLES

ÖZET

Yeni DNA Polimeraz Gama İnhibitörü Tarafından MLH1 Eksik Kolon Kanseri Büyümesinin Seçici İnhibisyonu

DNA onarım yolları arasındaki sentetik ölümcül etkileşimler kanser hücrelerini seçici oalrak öldürmek için önemli bir stratejidir. Yanlış eşleşme onarım (MMR) proteini MutL homolog 1 (MLH1) ve mitokondriyal baz eksizyon onarım proteini DNA polimeraz γ (Pol γ) arasındaki sentetik lethalite etkileşimi, bu çalışmada MLH1 eksikliği olan kanserlerin seçici tedavisi için kullanılmıştır. *MLH1* genindeki germline mutasyonları ve anormal *MLH1* promotör metilasyonu, polipsiz kolorektal ve endometriyal kanserler dahil olmak üzere birçok kanser oluşum riskinin artmasıyla sonuçlanır. *MLH1* eksikliği olan kanser hücrelerinde Pol γ inhibisyonu sentetik letal seçicilik sağladığından, MLH1 eksikliği olan kanser hücrelerini seçici olarak öldüren yeni Pol γ inhibitörleri için çeşitli veri tabanlarından ve kimyasal ilaç kütüphanesi moleküllerinden kapsamlı bir küçük molekül taraması gerçekleştirdik. Bu Pol γ inhibitör moleküllerini *in vitro* ve *in vivo* olarak karakterize ettik ve Pol γ proteinine yüksek afiniteli bir bağlayıcı ve *in vitro* ve *in vivo* Pol γ zincir yer değiştirme ve tek nükleotid doldurma DNA sentez aktivitelerinin güçlü bir inhibitörü kongo kırmızısı (CR) (3,3'-[(1,1'-Bifenil)-4',4'-diyl) bis(azo)] bis [4-amino-1-naftalensülfonik asit]; Zinc03830554)'i tanımladık. CR, MLH1 eksikliği olan HCT116 insan kolon kanseri hücrelerinin hücre proliferasyonunu azalttı ve HCT116 ksenograft tümör büyümesini baskılarken, MLH1 içeren hücre proliferasyonunu ve ksenograft tümör büyümesini etkilemedi. CR, Pol γ aktivitesini ve oksidatif mitokondriyel DNA (mtDNA) hasar onarımını inhibe ederek, MLH1 eksikliği olan hücrelerde reaktif oksijen türlerinin üretimini ve oksidatif mtDNA hasarını artırarak mitokondriyel disfonksiyona ve hücre ölümüne neden oldu.

Anahtar Sözcükler: MLH1 eksikliği olan kolon kanseri, yanlış eşleşme onarımı, polimeraz gama, sentetik letalite, kongo kırmızısı

ABSTRACT

Selective Inhibition Of MLH1 Deficient Colon Cancer Growth By Novel DNA Polymerase Gamma Inhibitor

Synthetic lethal interactions between the DNA repair pathways is an important strategy to preferentially kill cancer cells. The synthetic lethal interaction between the mismatch repair (MMR) protein, MutL homolog 1 (MLH1), and in the study the mitochondrial base excision repair protein, DNA polymerase γ (Pol γ) was used for the selective treatment of MLH1 deficient cancers. Germline mutations in the MLH1 gene and abnormal MLH1 promoter methylation result in an increased risk of many cancers, including nonpolyposis colorectal and endometrial cancers. As Pol γ inhibition in MLH1-deficient cancer cells confers synthetic lethal selectivity, we performed a comprehensive small molecule screening from several databases and chemical drug library molecules for novel Pol γ inhibitors that selectively kill MLH1-deficient cancer cells. We characterized these Pol γ inhibitor molecules *in vitro* and *in vivo* and found that a high-affinity binder to Pol γ protein and a potent inhibitor of Pol γ strand displacement and single nucleotide filling DNA synthesis activities *in vitro* and *in vivo*, congo red (CR) (3, 3'-[(1,1'-Biphenyl)-4',4'-diyl) bis(azo)] bis [4-amino-1-naphthalenesulfonic acid]; Zinc03830554). CR reduced cell proliferation of MLH1-deficient HCT116 human colon cancer cells, and while HCT116 suppressed xenograft tumor growth, it did not affect MLH1-proficient cell proliferation and xenograft tumor growth. CR caused mitochondrial dysfunction and cell death by inhibiting Pol γ activity and oxidative mitochondrial DNA (mtDNA) damage repair, increasing the production of reactive oxygen species and oxidative mtDNA damage in MLH1-deficient cells.

Keywords: MLH1-deficient colorectal cancer, mismatch repair, polymerase gamma, synthetic lethality, congo red

INTRODUCTION AND AIM

2.1 DNA Damage

The human genome occurs in two separate genomes nuclear and mitochondrial. The nuclear genome has 6 billion bases and codes for about 25000 protein genes, whereas the mitochondrial genome is a circular plasmid with about 17000 bases and codes for 37 genes(1). The mitochondrial genome is separated from the nuclear genome, which encodes for 13 polypeptides, 22 transfer ribonucleic acids (tRNAs), and two ribosomal ribonucleic acids (rRNAs) involved in oxidative phosphorylation. Superoxide (O_2^-), hydrogen peroxide (H_2O_2), and hydroxyl radicals ($OH^\cdot$) produced by mitochondrial respiration cause damage to mitochondrial DNA (mtDNA)(2). If mtDNA damage accumulates, it can cause mitochondrial dysfunction and the activation of particular signaling pathways, which can result in senescence, cell death, or uncontrolled proliferation(1).

The number of DNA damages per cell every day is estimated to be around one hundred thousand(1,3). DNA damage is categorized to sources exogenous and endogenous. It is critical to assess the diverse types of DNA damage induced by these sources to comprehend the DNA repair systems that repair these damage(4,5). While radiation, dietary habits, and environmental pollutants are examples of exogenous DNA damage, endogenous sources include reactive oxygen species (ROS) produced by the electron transfer chain (ETC) mechanism, and structural modifications such as depurination or depyrmidination, and spontaneous mistakes during DNA replication(6,7). Base lesions, single-strand breaks (SSBs), double-strand breaks (DSBs), and inter-strand crosslinks (ICLs) are all examples of exogenous and endogenous DNA damages which can cause genomic instability.

Major base lesions are shown in table 1. Cytosine and 5-methyl cytosine are the most frequently deaminated bases(3,8). The most prominent of the ROS species are O_2^-, H_2O_2, and OH are byproducts of the ETC during cellular respiration(9). The OH radical induces the opening of an imidazole ring in guanine and adenine to form the

cleaved purine structure formamidopyrimidine(10). The saturated imidazole ring 7,8 dihydro-8-oxoguanine (8-oxo-G) is another biologically important and substantial oxidative base lesion produced by hydroxylation of the C-8 residue of guanine. ROS can impair the DNA backbone by generating single-strand breaks in mammalian cells, in addition to damaging DNA bases(11). Ionizing radiation (IR) and ROS produce a similar spectrum of base lesions, which form a cluster of highly reactive OH by radiolysis of the surrounding water. N7-methylguanine, N3-methyladenine, and O^6-methylguanine are methyl lesions created by S-adenosylmethionine (SAM), which is used as a methyl donor by methyl transferases during typical methylation processes(6). The electrophilic alkylating agents bind to the highly nucleophilic base ring nitrogen with a stronger affinity. Modified adenine (N1, N3, N6, and N7), guanine (N1, N2, N3, N7, and O6), cytosine (N3, N4, and O2), thymine (N3, O2 and O4), and alkyl phosphates in the DNA backbone are examples of adducted DNA bases(10,12).

Table 1. Major DNA Base Lesions.

Normal Bases	**Deaminated DNA Bases**	**Oxidized DNA Bases**	**Methylated DNA Bases**
Adenine	Hypoxanthine	Formamidopyrimidine	N^3-methyladenine
Guanine	Xanthine	7,8 dihydro-8-oxoguanine	N^7-methylguanine O^6- methylguanine
Cytosine	Uracil		N3-methylcytosine
Thymine	5-methylcytocine	Thymine glycol	O^4- methylthymine O^4- ethylthymine N^3- methylthymine

2.2 DNA Repair Pathways

The DNA damage response (DDR) is a genome-wide monitoring system that protects cells from potentially mutagenic DNA damages originating from both endogenous and exogenous sources. Lesion-specific sensor proteins trigger a DDR after the DNA has been damaged. The DDR usually works by coordinating the actions of DNA repair and checkpoint systems to stimulate DNA damage repair before replication or to activate cell death pathways when there is too much damage(4,13–15).

In mammalian cells, there are different DNA repair pathways. Base excision repair (BER), nucleotide excision repair (NER), mismatch repair (MMR), and double-strand break repair (DSBR) are all important DNA repair processes in mammalian cells(13). While the BER pathway repairs oxidative, deamination, alkylation, and abasic single base damage to the DNA helix, the single-strand break repair (SSBR) and DSBR pathways repair breaks in the DNA backbone(9). SSBs are usually triggered by oxidative DNA damage, abasic sites, or incorrect DNA topoisomerase 1 (TOP1) activity(16,17). Irresolvable SSBs cause Poly (ADP-ribose) polymerase (PARP) activation, which releases cellular nicotinamide adenine dinucleotide (NAD^+), adenosine triphosphate (ATP), and apoptosis-inducing factor (AIF) in cells(18,19). The SSBR pathway can be either short-patch (SP) or long-patch (LP). While SSBs are transiently identified by PARP in the long patch SSBR pathway, apurinic/apyrimidinic (AP) endonuclease (APE1) recognizes SSBs generated during the BER in the short patch SSBR pathway, and each other similar end-processing pathway is realized(20–22).

BER pathway is well known in the nucleus, where it is most active during the G1 phase, and was the first repair pathway discovered in the mitochondria. To repair DNA with abasic sites or base damage, BER has four enzymes: glycosylase, endonuclease, polymerase, and ligase (Figure 1). BER process starts by the DNA glycosylase catalyzes the breakage of the N-glycosidic bond between the damaged base and its deoxyribose, resulting in an abasic site(23–25). In mammals, there are a total of ten DNA glycosylases. Depending on whether they have an intrinsic lyase activity, these enzymes can be classified as monofunctional or bifunctional. For encoding DNA glycosylases nuclear genes are responsible and some of them include a mitochondrial targeting signal that allows for mitochondrial translocation. Monofunctional DNA glycosylases are uracil DNA glycosylases (UDG), N-methylpurine DNA Glycosylase (MPG), and MutY Homolog (MUTYH), when bifunctional DNA glycosylases with a glycosylase and an additional lyase activity are Nth-like DNA glycosylase 1 (NTHL1), Nei-like DNA glycosylase 1 (NEIL1) and Nei-like DNA glycosylase 2 (NEIL2)(26–28). This lyase activity cleaves DNA strands via β- or βδ- elimination. The 3′/5′-end structures that follow from β-elimination and βδ-elimination are 3′-phospho-α,β-

unsaturated aldehydes (3′-PUA)/5′-P and 3′-P/5′-P, respectively. These occurred 3′-end structures can't be used as primers for DNA polymerases' DNA-repair synthesis, therefore APE1 or polynucleotide kinase/phosphatase (PNKP) are needed to create 3′-OH termini(29).

Next step, cleavage of AP sites to produce 3′-OH/5′-dRP termini, as well as hydrolyzing 3′-phosphodiester bonds in 3′-PUA to produce 3′-OH by APE1 which appears to be the sole active endonuclease in mammals. APE1 creates 3′-OH ends in both processes, which are essential for DNA polymerases to repair DNA. These 3′-end compounds, such as 3′-PUA and 3′-phosphoglycolate, are easily removed by APE1. On the other hand, APE1 has relatively little activity on substrates that include 3′-phosphates. PNKP, rather than APE1, has been demonstrated to be effective at removing 3′-phosphate. APE1's incision of AP sites produces not only 3′-OH but also 5′-dRP, which must be eliminated before the BER reaction can proceed. By β-elimination, DNA glycosylases with intrinsic AP lyase activity eliminate the 5′-dRP moieties. The DNA polymerases have an intrinsic activity to remove 5′-dRP in addition to DNA glycosylases(29,30). This process is catalyzed by hydrolysis and generally needs the presence of magnesium (Mg^{2+}) as a cofactor. The dRP or AP sites can be oxidized or reduced. Flap structure-specific endonuclease 1 (FEN1) may recognize the 5′-flap end structure and cut the nucleotide a few bases downstream of the 5′-dRP when AP sites are changed by oxidation/reduction (31).

The DNA polymerases remove the dRP and fills in the single nucleotide gap created by the removal of the lesion base in the pathway's third step. In the nuclear BER(nBER) pathway, DNA polymerase β (Pol β) and in mitochondrial BER (mtBER) pathway Pol γ is used (32). In the final step, the DNA ligase interacting strongly with X-ray repair cross-complementing protein 1 (XRCC1) seals the nick that results from single nucleotide incorporation(28). DNA polymerases and ligases have been shown to enhance the efficiency of the entire BER reaction when they interact with other BER proteins(29).

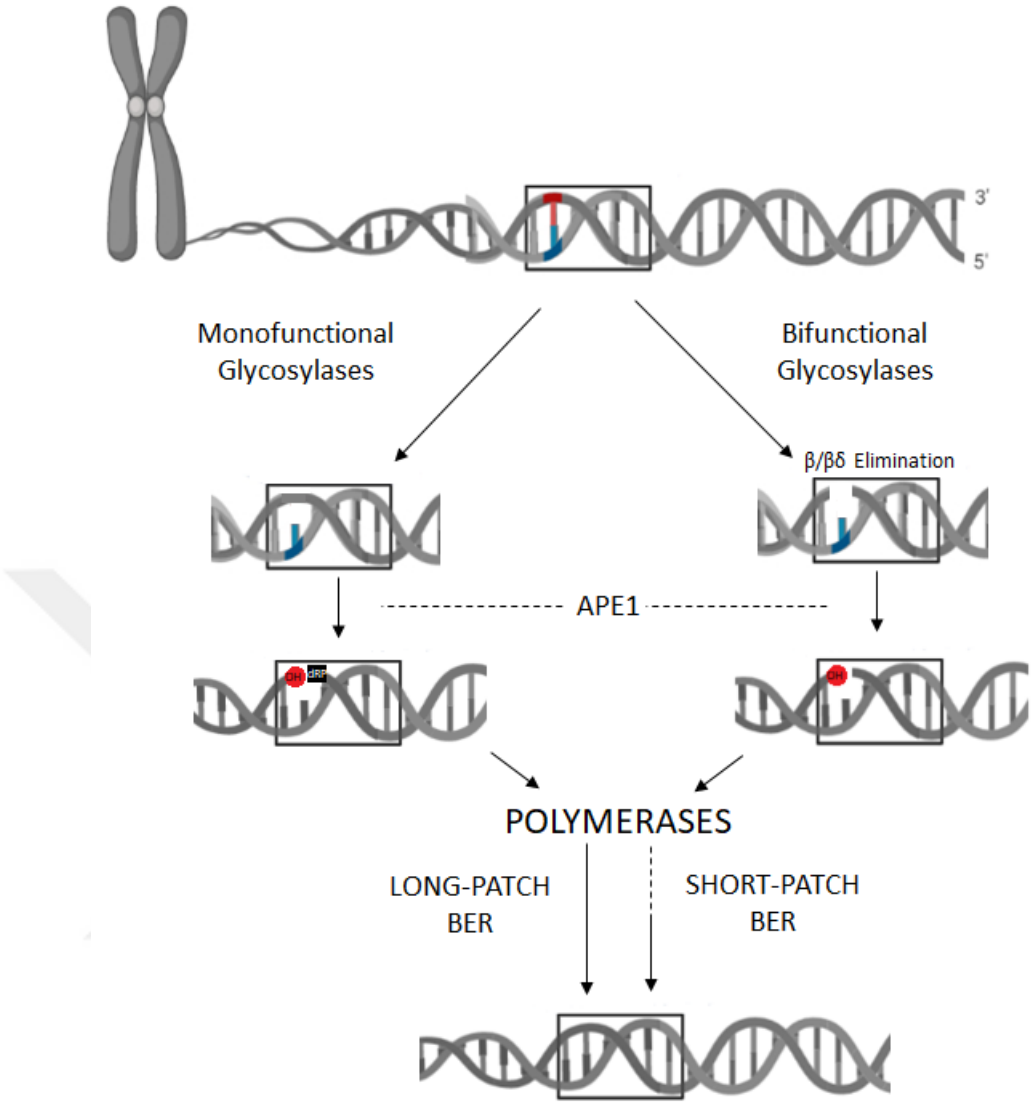

Figure 1. Basic Base Excision Repair Schema. The 3′ or 5′-intermediates formed during abasic site processing are shown in red and black, while the newly incorporated single nucleotide (in SP-BER) or repair patch (4–6 nt in LP-BER) is shown in the adjacent form.

NER is the preferred method for removing bulky lesions caused by ultraviolet radiation, benzo[a]pyrene adducts, or chemotherapeutic drug damage, and it is exclusively found in the nucleus(33). Transcription-coupled repair (TCR) and global genome repair (GGR) are two sub-pathways of NER(34). NER is more complicated than BER. DNA damage recognition in TCR-NER and GGR-NER is achieved by the Cockayne Syndrome Group B/Group A (CSB/CSA) protein and Xeroderma

Pigmentosum Complex (XPC) protein, respectively. However, the most significant distinction between GGR-NER and TCR-NER includes the processing of the RNA polymerase. Damage recognition in TCR-NER is thought to occur when it detects damage in the transcribed strand by blocking or arresting the RNA polymerase complex. Many of the events that follow in the pathway are similar in both NER sub-pathways(29,33,35,36).

MMR is an evolutionarily conserved process that contributes to replication fidelity by repairing post-replicative base mismatches and insertion-deletion loops (IDLs) within repetitive DNA sequences that have originated from strand slippage events. The nucleotide mismatch is detected in MMR's first step by the heterodimeric MutS homolog (MSH) complex. Then, MutL homolog 1 (MLH1)/ MutL homolog 4 (MLH4) and MLH1/ MutL homolog 3 (MLH3) complexes immediately move to the mismatch lesion location and connect to the DNA molecule, forming a sliding clamp. Several proteins come together to execute nucleotide excision and resynthesis functions(37,38). Finally, the remaining nick is ligated by DNA ligase.

All of BER, NER, and MMR pathways can be used to repair single-strand breaks(39). NER is only present in the nucleus, whereas MMR components have also been detected in mitochondria and are thought to help in mtDNA repair(1). MMR deficient tumor cells have a considerably higher mutation rate than normal cells. Patients with Lynch syndrome are caused by mutations in the MMR genes *MLH1* and *MSH2*(40,41). Also, Lynch syndrome is a hereditary cancer syndrome that is linked to a genetic propensity to a variety of cancers with MMR deficiency. The mtBER pathway repairs DNA damage produced by chemotherapeutic agents in cells with MMR deficiency, ensuring cell survival(42).

2.3 DNA Polymerase γ Protein

Mammalian DNA polymerases are classified into four families based on sequence homology: A, B, X, and Y. Members of the A DNA polymerase family, of which the DNA polymerase γ (Pol γ) is a family member, share homology with *E. coli* DNA

polymerase I, which is encoded by the *Pol A* gene. A family of DNA polymerases is involved in DNA lesion bypass and mitochondrial DNA replication and repair(43–45).

In the early 1970s, Pol γ was first described as a novel RNA-dependent DNA polymerase activity in eukaryotic cells. DNA Pol γ is a critical element of mitochondrial DNA, as it is important for mtDNA replication and repair. The Pol γ structures are revealed information on how the enzyme can change its processivity and integrity to be efficient at both replication and repair.

2.3.1 Structure

Pol γ enzyme is part of the unique mechanism involved in both replication and repair of mtDNA. The Pol γ is found in mitochondria as a complex consisting of a catalytic subunit (pol γA, 140 kDa) and a dimeric form of its accessory subunit (pol γB, 55 kDa). The Pol γA occurs in an N-terminal exonuclease domain, a connecting linker region, and a C-terminal polymerase domain(46,47). The Pol γA has several enzymatic activities, comprising polymerase activity, the 3'-5' proofreading ability, and 5'-dRP lyase activity(48).

The single Pol γA binds asymmetrically with a Pol γB dimer, also the Pol γA is associated with a subdomain known as the accessory interacting domain (AID) that extends around Pol γB as shown in figure 3(49).

The Pol γB is known to promotes DNA binding and processive DNA synthesis. During replication complex formation, Pol γB turns towards Pol γA without changing the proximal domain between the two subunits (Fig 2). In this configuration, Pol γB is closer to the substrate. The interaction between the two subunits provides a dynamic contribution to mechanisms of the polymerase activity and the exonuclease activity.

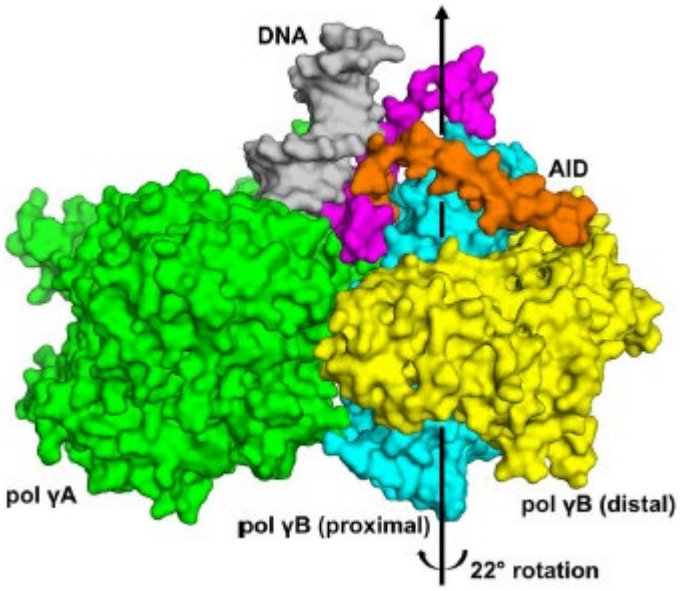

Figure 2. Domain organization of Pol γ (PDB ID:3IKM)

2.3.2 Function

The Pol γ is critically important for mtDNA replication and maintenance and Pol γ mediated defects result in the loss of cellular respiration and finally induce mitochondrial genetic diseases.

Pol γ cooperates with many proteins for mtDNA replication. Pol γ cannot use double-stranded DNA (dsDNA) as a template, and therefore, during mtDNA replication, a DNA helicase is required to unwind the dsDNA template. The topoisomerase enzyme, which is necessary for the mtDNA unwinding, displays enzymatic activity on the phosphodiester backbones of the mtDNA chain, allowing the positive supercoils to lose. The hexameric Twinkle helicase occurs in a fork structure together causing mtDNA duplex denaturation. Twinkle loads Pol γ to a single-stranded 5'-DNA loading domain of the fork and travels in front of Pol γ. Mitochondrial single-stranded DNA (ssDNA) binding protein (mtSSB) binds to ssDNA for preventing secondary structure formation and stabilization during mtDNA replication. Mitochondrial RNA polymerase (mtRNAP) and ribonuclease H1 (RNaseH1) are required for RNA primer formation and removal to initiate DNA replication at the 3'-

end(50–53). Pol γ works with together mitochondrial genome maintenance exonuclease 1 (MGME1), Flap structure-specific endonuclease 1 (FEN1), and mitochondrial DNA ligase III (mtLigIII) to seal DNA nicks during Okazaki fragment processing or LP-BER (Fig 3)(54,55).

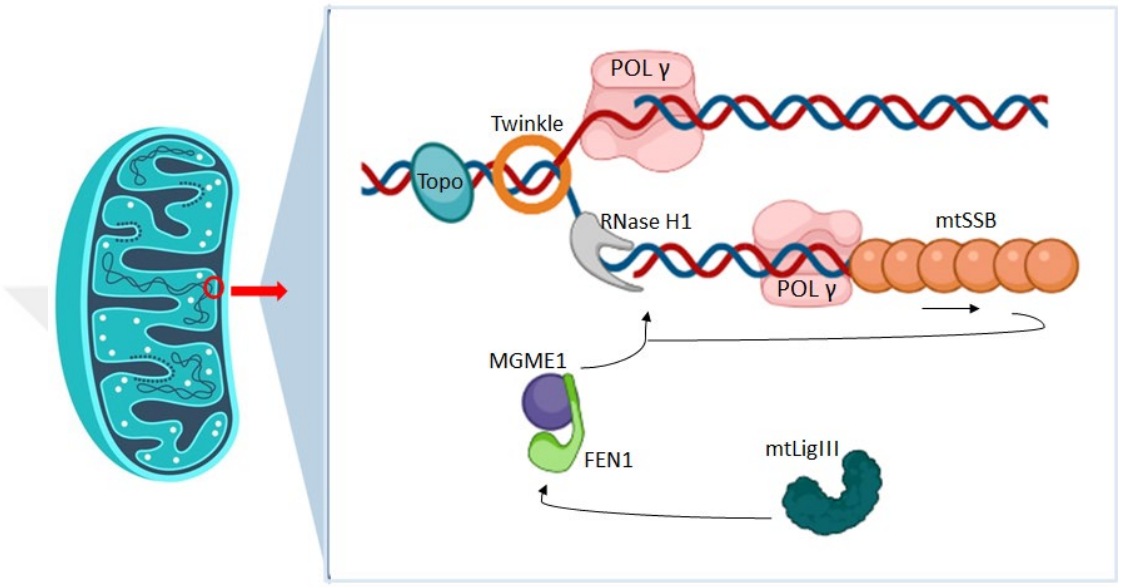

Figure 3. mtDNA Replication. The way arrowed in replication fork is indicated control region including the heavy-strand origin of replication and other strand is indicated he displacement-loop (D-loop); Blue, Topoisomerase; Orange, Twinkle; Pink; Polymerase gamma; Grey, Rnase H1; Purple, MGME1; Green, FEN1; Dark Green, Ligase.

The exonuclease enzymatic activity can proofread ability for the polymerase, and enhances the accuracy of its DNA synthesis by excising incorrectly polymerized nucleotides. The 3'-5' exonuclease activity of Pol γ shows a preference for dsDNA containing 3'-terminal mispairs.

Another role of Pol γ is 5'-dRP lyase activity in mtBER (Fig 4)(56). The first step of mtBER is the catalyzed reaction of DNA glycosylases, which recognize the oxidative DNA lesion and cleave the N-glycosidic bond, and resulting in the formation of an abasic region(57). 8-oxoguanine DNA glycosylase-1 (OGG1) and UDG are two of the most study and well-known significant mtDNA glycosylases. Both

mitochondrial and nuclear isoforms of the same DNA glycosylases have different alternative transcription initiation sites and alternative splicing patterns(58). To repair the formed abasic region, the APE1 isoform of APE, which is involved in both nBER and mtBER processes, has evolved(9). It has been demonstrated that APE1 activity is higher in mitochondrial fractions than in nuclear fractions(59). After APE1 has processed the AP site, Pol γ inserts the correct nucleotide(s) into the generated gap. To the elimination of the 5' terminal dRP sugar moiety required for nucleotide gap filling in mtBER, Pol γ provides an intrinsic dRP lyase activity mechanism. There are two different BER subpathways depending on whether Pol γ inserts one or more nucleotides; however, it is unclear why the pathway proceeds through the SP-BER or LP-BER(60). The mtBER nick sealing step is catalyzed by mtLigIII, a unique protein that functions in both replication and repair. mtBER is completed with this final step(56,61,62).

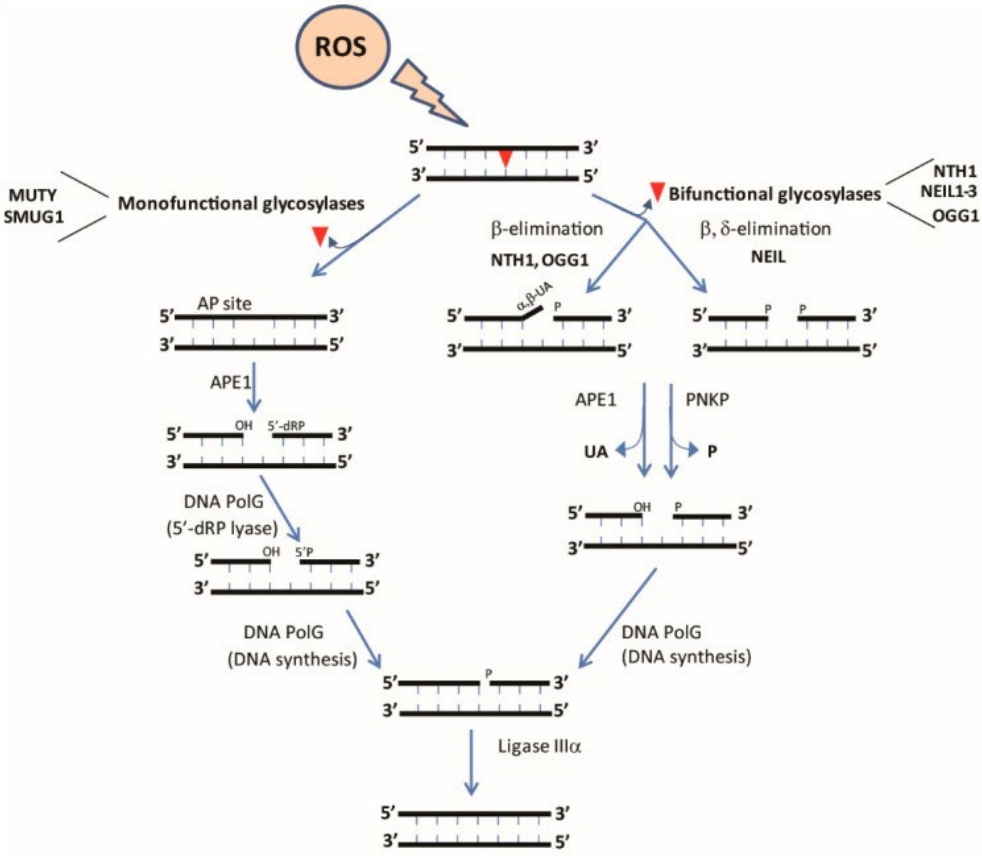

Figure 4. BER pathway steps in the mitochondria (CC by 4.0) (56).

2.4 DNA Polymerase γ Inhibitors In Cancer Cells

Pol γ is responsible for all mechanisms of replication, recombination of the mitochondrial genome, and repair of mtDNA damage. Therefore, the mechanisms selectively inhibit Pol γ activities is an intriguing research topic. Extant studies show that Pol γ has been to be highly susceptible to inhibition by agents such as 3'deoxy-3'azidothymidine triphosphate (AZT-TP), dideoxynucleotides (ddNs), and other antiviral nucleotide analogs.

Nucleoside reverse transcriptase inhibitors (NRTI) are the basis of antiretroviral therapy the United States Food and Drug Administration (FDA) approved and clinically successful for controlling the human immunodeficiency virus 1 (HIV-1) infection. NRTIs can cause accumulated defects in the mitochondrial genome, mitochondrial dysfunction with mtDNA depletion, and alter mitochondrial energy hemostasis as a result of inhibition of Pol γ. AZT is a successful NRTIs drug that exhibited viral suppression. The analysis of AZT-TP the active form of the AZT drug showed that it is an inhibitor of both nuclear DNA (nDNA) Pol α, β, δ, ε, and mitochondrial Pol γ(63,64).

Research was shown that NRTIs such as AZT and ddNs cause mitochondrial-associated side effects such as myopathy and peripheral neuropathy. Experiments *in vitro* and *in vivo* revealed that extended ddNs exposure led to disrupted mitochondrial cristae in the damaged neurons, along with decreased action potentials. The toxicity of ddNs was found especially decrease mtDNA copy number in muscle samples(64–67).

It has been determined in cellular toxicity studies that menadione has an inhibitory effect on Pol γ in the mitochondrial matrix by passing through the mitochondrial membrane. Sasaki et al. determined that especially menadione showed strong anticancer effects compared to doxorubicin, cisplatin, and taxol in many radiations resistant cancer cell lines(68,69). In the continuation of this study, it was proved that menadione selectively increases the redox cycle and inhibits mtDNA replication activity by interacting with Pol γ.

2-benzoyl-6-(2,3-dimethoxybenzylidene)-cyclohexanol (AS13), identified in recent studies, shows a potential therapeutic effect like the anticancer drugs menadione and motexafin. AS13 has been shown to cause genetic instability in both MLH1-proficient and MLH1-deficient cells by producing ROS. Particularly, oxidative stress-mediated DNA damage was shown to repair only MLH1-proficient cells and cause cytotoxicity in MLH1-deficient cells with MLH1-selective effects of AS13(70). All of these studies provide new therapeutic hopes for the treatment of cancers associated with DNA repair proteins. However, more detailed research is needed because induced damage may promote cancer progression.

2.5 Targeting DNA Repair/BER Pathways For Cancer Treatment Using Synthetic Lethality

Chemotherapy, radiation therapy, and surgery are examples of traditional cancer treatments that are generally acknowledged and practiced. The structure and method of action of the chemicals used in cancer therapy differ widely, but they can cause significant toxic side effects, which compromise the therapeutic outcomes. DNA repair pathways act to maintain genomic integrity across DNA damage, which is caused by chemotherapeutic agents and radiation therapy. Successful cancer treatment is dependent primarily on the development of drugs that selectively destroy cancer cells while causing no harm to healthy cells(4,71).

Cancer is a disease of DNA repair that originates from mutation in the DNA. Multiple DNA repair processes are required for cancer cells to replicate their DNA and grow, which is the fundamental characteristic of cancer. As a result, cancer cells developed DNA-repair machinery that acts against cancer treatment(68,72). Therefore, the targeted therapy must include a combination of drugs or a single drug that causes DNA damage while blocking DNA repair pathways. Synthetic lethal interactions based on DNA repair can be used to obtain this selectivity. Synthetic lethality is defined as a type of genetic interaction that results in cellular death when two genetic events occur at the same time. In other words, synthetic lethality takes advantage of inter-gene interactions, in which the loss of another of two related genes

is nonlethal, but the loss of both causes cell death(73,74). As shown in Figure 5, synthetic lethality indicates that both genes must be altered to cause cell death. If either of these genes is activated, however, the cell's vitality can be maintained(75).

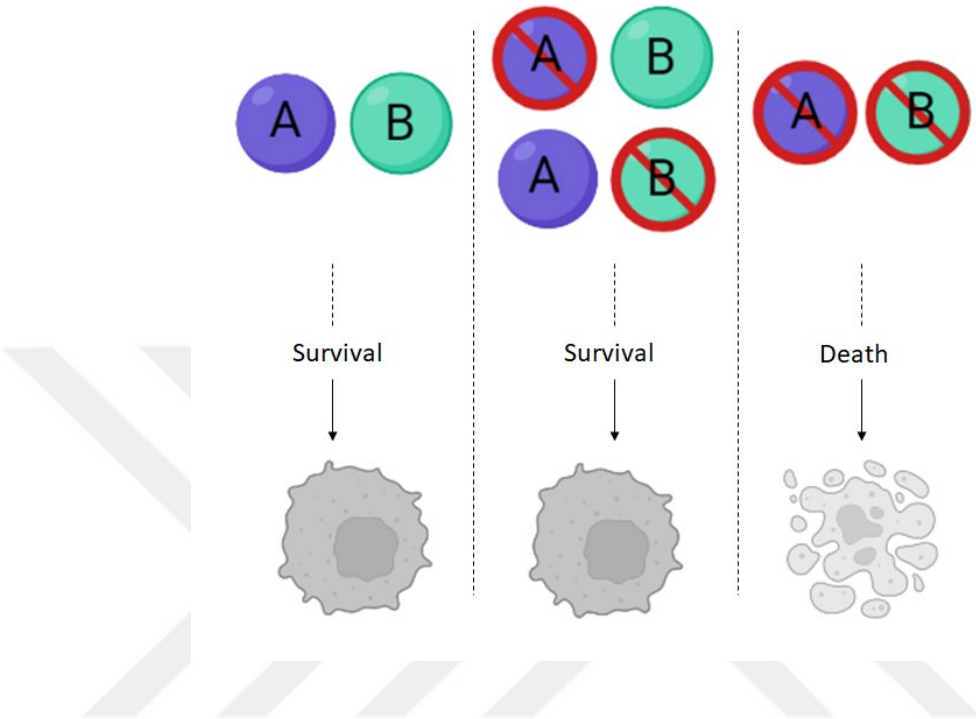

Figure 5. Synthetic Lethal Relationship Schema. Synthetic lethality: Loss of either gene/protein A or B in isolation is compatible with cellular viability, but a loss of both genes/proteins together results in cellular dead. Adapted from Nijman S, 2011(75).

Because many DNA repair genes are associated with oncogenes and tumor suppressor genes, they become potential targets for cancer therapy by using the synthetic lethality strategy. Many tumor suppressor and oncogene genes are tissue-specific as well. The most famous example is mutations in the tumor suppressor gene BRCA 1/2, which are known to cause breast and ovarian cancer but rarely other cancer types(71). In the following chapters, we would go over how to use a target-specific lethality method on tumor suppressor gene mutant tumor cells.

2.5.1 Synthetic lethal interaction between PARP1 and BRCA 1/2

The synthetic lethality link between breast cancer gene (*BRCA*) mutation and PARP1 inhibition is the best-studied(71). PARP1 is involved in the SSBR pathway that is connected to BER. PARP inhibition is thought to induce endogenously generated SSBs to persist, causing replication fork collapse and the generation of lethal DSBs. How PARP1 is inactivated may have an impact different on biological consequences. Interestingly, it was determined that PARP1 knockdown mediated by short interfering RNA (siRNA) does not cause considerable cytotoxicity in BRCA-deficient cells, but small-molecule inhibition causes SSB accumulation after alkylating agent treatment and is synthetically lethal in BRCA-deficient cells(76).

BRCA 1 and *BRCA 2*, which are mutated in an inherited cancer tendency that increases susceptibility to breast and ovarian cancers, have long been known to act as tumor suppressors. The homologous recombination (HR) DNA repair mechanism is influenced by both *BRCA* gene products. Loss of efficient HR results in DSB accumulation and cell death in BRCA-deficient cells. Because heterozygosity at a *BRCA* allele is linked to effective HR, DSB accumulation produced by PARP inhibition occurs specifically in tumor cells that have acquired $BRCA^{-/-}$ homozygosity. This approach has been reported by highly influential studies of cancer cells with BRCA1/2 dysfunction indicating that they were more sensitive to top PARP inhibitors than cells with normal BRCA function(42,76). The FDA has approved olaparib, a PARP inhibitor, for the treatment of clinical cases that, have harmful germline *BRCA* mutations(77).

2.5.2 Synthetic lethal interaction between MLH1 and DNA polymerase γ

BER and MMR can process 8-oxo-G base lesions caused by metabolic ROS. Recent research suggests that interactions between the BER and MMR DNA repair pathways may hold the potential for synthetic lethality in hereditary non-polyposis colorectal cancer (HNPCC) linked to *MLH1/MSH2*. *MLH1* and *MSH2* are thought to function as classic tumor suppressor genes, with tumor cells losing all *MSH2* or *MLH1*

functions but retaining at least one functional allele(40,78,79). A synthetic lethal screen revealed a link between the deletion of these MMR components, *MLH1* and *MSH2*, and DNA polymerases γ and β(79). Martin et al. demonstrated that MLH1 can localize to the mitochondria and that siRNA inhibition of several mitochondrial genes, including Pol γ and phosphatase and tensin homolog (PTEN)-induced kinase 1 (PINK1), can induce synthetic lethality in MLH1-deficient cells(42,80). The oxidative DNA lesions in the mtDNA can be increased as a result of this lethal synthetic interaction. In the case of MSH2/Pol β, 8-oxo-G accumulation was in the nDNA, whereas MLH1/Pol γ synthetic lethality occurred in an increase in mtDNA 8-oxo-G levels. Unrepaired base lesions can cause mutagenic GC→TA transversions and in both cases, the lethality might be repaired by silencing the adenine glycosylase MUTYH. DNA polymerase inhibitor, methotrexate is especially toxic to MSH2-deficient cells due to the induction of oxidative DNA damage(78,79,81,82). Methotrexate's role in HNPCC has not yet been thoroughly tested in the clinical setting, but DNA polymerase inhibitors are an intriguing possibility for HNPCC treatment(83).

Because MLH1 interacts with Pol γ, inhibiting Pol γ may be an effective way to specifically kill MLH1 deficient cancers. MLH1 is involved in both nuclear and mitochondrial genome repair. Pol γ is a mtDNA polymerase enzyme that is involved in the BER pathway and mtDNA replication. Although DNA repair pathways are specific to DNA lesions, there is some overlap in substrate specificity. The BER pathway is the most important for repairing oxidative DNA damage, but the MMR pathway also plays a role in repairing this damage. As a result, an inhibitor is required to specifically kill MLH1 deficient tumor or cancer cells while causing no harm to normal cells via Pol γ inhibition(42).

2.6 Aim Of Study

ROS is the primary cause of both nDNA and mtDNA damage. It has been reported that mtDNA mutations or defects in mtDNA coded protein syntheses can result in ROS

production(8,9,11). Pol γ plays a critical role in the repair process after mtDNA damage.

The inhibition of synthetic lethal associated specific DNA repair proteins is an effective target for selectively destroying tumor cells in cancers where the DNA repair pathway is inactive. The mtBER pathway repairs DNA damage caused by chemotherapeutic factors in colorectal cancer cells caused by *MLH1* gene damage, ensuring cell viability. It is possible to kill MLH1-deficient colorectal cancer cells by inhibiting Pol γ in the synthetic lethal interaction between MLH1 and Pol γ(42,77). There has yet to be identified in the literature an inhibitor with anticancer properties specific to the Pol γ protein. Using a molecular docking approach, we have previously shown that some small molecules bind directly to the Pol γ protein and also were optimized for the Pol γ synthesis activity reaction analysis.

In this PhD thesis project, we have characterized Congo Red (CR) (3,3'-[(1,1'-Biphenyl)-4',4'-diyl)bis(azo)]bis[4-amino-1-naphthalenesulfonic acid]; Zinc 03830554) , which has the highest tendency to bind to Pol γ protein among around 9500 small molecules according to our previous in silico study, *in vitro* and *in vivo* to investigate its effect on the selective treatment of MLH1-deficient colon cancer growth (Figure 6).

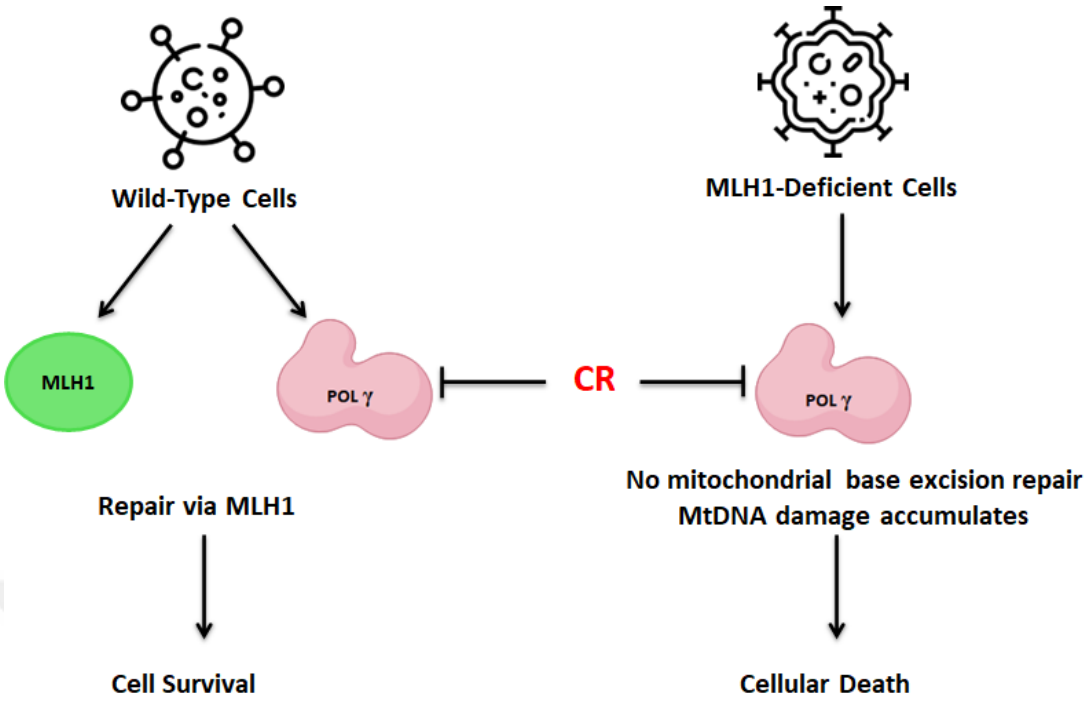

Figure 6. Schematic Explain of Our Study Aim. A schematic is illustrated that the loss of the Pol γ protein is compatible with cellular viability in MLH1-proficient cells, but CR inhibiting Pol γ results in the death of MLH1-deficient cells.

For the functional characterization of the novel Pol γ inhibitor CR, we performed the Pol γ enzyme activity assays. Then we have investigated the effects of CR on the proliferation of MLH1-deficient and MLH1-proficient colon cancer cells. Finally, nude mice xenograft studies were performed to investigate whether CR inhibits the growth of MLH1-deficient HCT116 and MLH1-proficient Lovo colon cancer tumors *in vivo*.

3. MATERIALS AND METHODS

3.1 Molecular Docking And Surface Plasmon Resonance Analysis

Three-dimensional coordinates of the X-ray crystal structure of the human Pol γ holoenzyme (protein data bank identification code (PDB ID): 3IKM) were selected as the receptor models in docking programs. The binding models for Pol γ inhibitors were predicted by using GOLD (GOLD Suite v5.2.2) on a Windows server equipped with an Intel Core i7-4600U processor (2.7 GHz) and 8 GB of RAM. The library used in molecular docking was composed of about 8550 plant secondary metabolites that provide 3D structures that we obtained from various online available databases: KEGG phytochemical compounds (https://www.genome.jp/kegg-bin/get_htext?br08003.keg), Analyticon-discovery MEGxp pure natural plant products (https://ac-discovery.com/purified-natural-product-screening-compounds), seaweed metabolites database (SWMD) (https://www.swmd.co.in), indofine chemicals (https://indofinechemical.com), Indian plant anticancer compounds database (InPACdb) (http://www.inpacdb.org), zinc database (https://zinc.docking.org), zinc natural products (https://zinc15.docking.org/substances/subsets/natural-products), and zinc database FDA approved drugs (http://zinc.docking.org/substances/subsets/fda). Docking of molecules was performed using the GOLD software and the hit molecules were evaluated according to the binding free energies (-10 ≤ kcal/mol).

Surface Plasmon Resonance (SPR) studies were performed as a service by Prof. Aykut Uren's group at Georgetown University, USA(84). Human recombinant Pol γ protein (Chimarx, USA) was immobilized on Biacore T100 CM5 sensor chips (GE Healthcare, Piscataway, NJ, USA), and 1200 small molecules from the Prestwick Chemical Library (http://www.prestwickchemical.com) were injected at a single concentration for initial screening. The relative binding of each compound (response units, RU) to Pol γ and RNA helicase A were normalized to analyte binding capacity (Rmax), which was taken as 100%. In addition, 7 different concentrations of the small molecules from in silico screening with calculated binding free energies around -10

kcal/mol were injected over the surface in triplicates. The small molecules were synthesized as a service and purchased from Ambinter (www.ambinter.com). SPR sensorgrams and dissociation constants (KD) values were obtained using Biacore T100 software.

3.2 Strand Displacement DNA Synthesis And Gap Filling Assays

3.2.1 Oligonucleotides and ^{32}P-labeling DNA substrate

The 51 mer duplex oligodeoxynucleotide containing one nucleotide (1-nt) gap substrate at position 26 has been used for the understanding of Pol γ activities. The oligonucleotides sequences are shown in Table 2. The sequences of the oligodeoxynucleotides used in this study were procured from DNA Technology A/S, Denmark.

Table 2. The Oligodeoxynucleotides Sequences

Substrate: Sequences
G1: 5'-GCTTAGCTTGGAATCGTATCATGTA-3'
G2: 5'-ACTCGTGTGCCGTGTAGACCGTGCC-3'
G3: 5'-GGCACGGTCTACACGGCACACGAGTGTACATGATACGATTCCAAG CTAAGC-3'

G1 substrate was 5' end-labeled using [γ-^{32}P] ATP using kinase reaction as the final concentration of 1 pmol/ µl oligodeoxynucleotide, 2 U T4 polynucleotide kinase (PNK), 1X T4 PNK Buffer and 1 µCi [γ-^{32}P] ATP. The mixture was incubated at 37 °C for 1 hour (h) and then was incubated at 60 °C for 20 minutes (min) for reaction inactivation.

3.2.2 Annealing reaction

For hybridized DNA substrate, the annealing reaction mixture was prepared 36 µl dH_2O, 2 µl of 1 M LiCl, and 2 µl of 20 pmol/µl oligonucleotide substrates and

incubated at 95 °C for 5 min. Then the heat block was turned off and let cool at room temperature over a period of 3-4 h to allow occur of the ^{32}P labeling dsDNA substrate with a 1-nt gap. The hybridized DNA substrates were stored at 4 °C.

3.2.3 Pol γ DNA synthesis activity

Pol γA catalytic subunit (140 kDa) and Pol γB accessory subunit (55 kDa) were expressed and purified from insect Sf9 cells and E. coli, respectively, as described previously (85)and provided by Dr. Whitney Yin from Texas University.

The measurement of Pol γ DNA synthesis activity is based on the principle of filling the gap by adding one or more nucleotides to the 1-nt gap containing the duplex DNA substrate of the Pol γ. To measure activity, radiolabeling duplex 51 mer DNA substrate with 1-nt gap was prepared in section 3.4.1.

The recombinant Pol γ protein was incubated with the increasing concentrations of CR on ice for 5 min in a reaction buffer (20 mM HEPES/KOH pH.7.5, 0.1 mg/ml BSA, 100 mM KCl, 1 mM β-mercaptoethanol, and 5 % glycerol). The synthesis reaction was initiated by the addition of 100 fmol/µl ^{32}P-labeled 1 nt-gap substrate, 5 mM $MgCl_2$, and 0.05 mM dNTPs to Pol γ. The reaction mixture was incubated at 37 °C for 20 min. The same reaction conditions were used for the 1-nt gap-filling assay, except dCTP was used instead of dNTPs. Then the reaction was stopped by the addition of an equal amount of the formamide loading dye (90 % formamide, 10 mM EDTA, 0.01 % bromophenol blue, and 0.01 % xylene cyanol) and incubated at 95 °C for 10 min. The samples were run on denaturing gel (20 % polyacrylamide-7 M urea) in 1X TBE buffer at 15 W for 2 h. Gels were visualized by PhosphorImager equipment (Typhoon FLA7000) and analyzed using the ImageQuant software (GE Healthcare Life Sciences, USA). The percent of each product with a given number of nucleotides incorporated is calculated as follows: % of total= (amount of radioactivity associated with each dNMP addition/total radioactivity) x 100. Values are corrected for background in the no enzyme control. IC_{50} value can be calculated.

3.3 Cell Culture

HCT116, LoVo, and SW48 colon cancer cell lines were purchased from ATCC, USA. HCT116VA (lacking *hMLH1*; vector alone) and HCT116V1 (transfected *hMLH1*) cell lines from Dr. Anatoly Zhitkovich, Brown University were obtained. All HCT116 cell types were grown in Dulbecco's Modified Eagle Medium: Nutrient Mixture (DMEM) (Life Tech, USA), 10 % Fetal Bovine Serum (FBS) (Life Tech, USA), and 1 % Penicillin/Streptomycin (Life Tech, USA) and also was added 400 µg/ml Geneticin Selective Antibody (Life Tech, USA) to same complete culture media for HCT116 VA and HCT116 V1 cells. All cells were grown in a humidified incubator (Thermo Scientific, USA) at 37 °C in 5 % CO_2.

3.4 Isolation Of Mitochondrial Isolation From Cell Culture

HCT116 VA and HCT116 V1 cells were seeded to the 150 mm dish plate with media properly as $5x10^7$ cells/plate. Cells were incubated with 50 µM CR in serum-free DMEM for 2 h at 37 °C, a 5 % CO_2 incubator. The treated and untreated cells were washed with PBS, harvested with trypsin/EDTA, and resuspended in MSHE buffer (210 mM mannitol; 70 mM sucrose; 10 mM HEPES, pH 7.4; 1 mM EGTA; 2 mM EDTA; 0.15 mM spermine; 0.75 mM spermidine; and 5 mM DTT) with protease inhibitor cocktail (Roche) added just before use, and homogenized with a Potter-Elvehjem glass/glass homogenizer. Before homogenization for isolation of both the mitochondrial and nuclear extracts, cells were mildly treated with digitonin to ensure plasma membrane permeabilization. The homogenates were centrifuged at 500xg for 12 min, and supernatants were centrifuged at 10,000xg for 10 min by transferring to new tubes. The pellet from the first centrifugation was incubated on ice for nuclear extract isolation. After 10,000xg centrifugation, the supernatant was removed, and the pellet was suspended in 3 % Ficoll400 prepared in MSHE buffer. The mitochondrial fraction was prepared by 6 % Ficoll gradient with the mitochondrial suspension and centrifuged 10,000xg for 30 min. Following centrifugation, the pellet which contained the mitochondrial layer and the nuclear-containing departed pellet was resuspended in an equal volume of buffer I (10 mM Tris-HCl pH 7.8, 200 mM KCl) and buffer II (10

mM Tris-HCl pH 7.8, 600 mM KCl, 2 mM EDTA, 40 % (v/v) glycerol, 0.2 % (v/v) NP-40, 2 mM DTT, 1X protease inhibitor cocktail (Roche)). The suspended pellets were sonicated at 3 times 5 sec pulses at 5 W, with a 55 sec interval, and incubated for 1.5 h at 4 °C on the shaker. Cell lysates were ultra-centrifuged at 130,000xg for 1 h and following the supernatant was dialyzed using Slide A Lyzer Mini Dialysis Equipment (Thermo Fisher Scientific, USA) against buffer III (25 mM Hepes-KOH pH 8.0, 100 mM KCl, 12 mM MgC12, 1 mM EDTA, 17 % (v/v) glycerol, 1 mM DTT, 1X protease inhibitor cocktail) for overnight at 4 °C. Finally, extracts were centrifuged at 16,000xg for 10 min. Protein concentration of both nuclear and mitochondria purified extracts was determined by the Bradford method (Bio-Rad Protein Assay, Bio-Rad Laboratories, Hercules,CA, USA) following the manual protocol.

3.5 Measurement Of Cell Extract One-Nucleotide Incorporation Activity

Single nucleotide gap-filling reactions were carried out using HCT116 mitochondrial and nuclear cell extracts, as previously described with a few changes(86). Single nucleotide gap-filling reactions were performed in a 10 µl reaction buffer (40 mM HEPES, pH 7.6, 0.1 mM EDTA, 5 mM $MgCl_2$, 0.2 mg/ml BSA, 50 mM KCl, 1 mM DTT, 40 mM phosphocreatine, 100 µg/ml creatine phosphokinase (Sigma-Aldrich, USA), 2 mM ATP (GE-Healthcare, USA), 40 µM of each dATP, dTTP, dGTP and 4 µM of dCTP (Roche Applied Sciences, USA), and 3 % glycerol) containing 100 fmol 1-nt gap substrate and 2 µCi of ^{32}P-dCTP (GE Healthcare, USA). The reactions were started by adding 0.5 g of mitochondrial and nuclear extracts and were incubated at 37 °C for 1 h. After the adding an equal volume of the formamide loading dye, reactions were incubated at 75 °C for 10 min. Samples were run on 20 % denaturing gel and were visualized as described above. The experiments were performed in duplicate. The incorporation of ^{32}P-dCTP activity was quantified as the increase in the signal intensity.

3.6 Western Blot Assay

Cell extracts containing equal protein amounts were mixed with loading buffer and denatured at 95 ºC for 5 min, and then run on a 4-12 % gradient SDS-PAGE (Thermo Fisher Scientific, USA) gel. After transferring the samples to a PVDF membrane (Bio-Rad, USA), were blocked with 5 % milk powder (Bio-Rad, USA) prepared in tris buffer solution (TBS-T) containing 0.1 % Tween-20 (Bio-Rad, USA). After this period, the membrane was incubated overnight at 4 ºC with the primary antibody of choice to confirm the purity of the mitochondrial and nuclear extracts. Primary antibodies used in this study: mouse anti-Lamin A/C (1:200, cat # NCL-LAM-A/C, Leica Biosystems), mouse anti-COX IV (1:1000, cat # A21347, Invitrogen), anti-MLH-1 (1:1000, cat # 4256, Cell Signaling, ABD), and anti-β-actin (1:1000, cat # 4967, Cell Signaling, ABD). After incubation, the membrane was washed 3 times with TBS-T solution for 5 min and incubated with anti-mouse IgG, HRP linked (1:5000, cat # 7076, Cell Signaling Technology) secondary antibody for 1 h at room temperature. After washing 3 times for 15 min in TBS-T solution, the membrane was exposed to Pierce ECL Plus according to the manufacturer's protocol (Pierce). The immunoblots were then visualized using ChemiDoc MP Imaging systems (Bio-Rad Laboratories).

3.7 Real-Time Cell Proliferation Assay Using The Xcelligence System

The xCELLigence real-time cell analysis (RTCA) system is a basic protocol to monitor alterations in cell adhesion following response to drug treatment. To the effects of CR on cell proliferation were measured using the RTCA system according to the manufacturer’s protocol. The wells in the E-plate 16 were added 100 µL DMEM, then the plate was placed in the RTCA DP station in the humidified incubator following incubation at room temperature for 15 min. In this step, the results of background reading were demonstrated in the presence of medium alone. HCT116VA and HCT116V1 cells were added to the wells with media properly as 15,000 cells/well in 90 µL. The serial dilutions of CR were added when cells come log phase. The assay was observed for 72 h with an interval 30 min. The IC_{50} values acquired with measurements were calculated by xCELLigence RTCA software.

3.8 Colony Forming Assay

HCT116 VA and HCT116 V1 cells were seeded in 6-well plates (500 cells/well) and treated with 5 μM CR. Colonies were allowed to grow for 10 days. Then, the plates were washed with 1X PBS, fixed with methanol, stained with 1 % methylene blue, and washed with 1X PBS to remove excess dye, air dried, and counted. Percent survival fraction was expressed as the ratio of plating efficiency (number of colonies formed/number of colonies were seeded) of treated cells to that of untreated control cells multiplied by 100.

3.9 Quantitative Analysis Of 8-Hydroxydeoxyguanosine (8-OHdG)

Mitochondria from treated and untreated HCT116 VA and HCT116 V1 cells were isolated as described above. mtDNA from isolated mitochondria was purified using a DNeasy kit (Qiagen). 8-hydroxydeoxyguanosine (8-OHdG) was determined by using Oxiselect Oxidative DNA Damage ELISA Kit (8-OHdG Quantitation; CellBioLabs) according to the manufacturer's instructions. Briefly, the assay plate was covered with 8-OHdG conjugate and incubated overnight at 4 ºC. After incubation, the coated plate was washed with dH_2O and was incubated by adding assay diluent at 4 ºC until use.

Each mtDNA sample was incubated by adding Nuclease P_1 (250 U/mL in 20 mM $C_2H_3NaO_2$, 5 mM $ZnCl_2$, 50 mM NaCl), 10 U of Alkaline Phosphatase solution, 10 U of $MgCl_2$ for 2 h at 37 ºC. After incubation, all DNA samples were centrifuged at 6,000xg for 5 min, and then the supernatant was transferred to a new tube. The coated plate was incubated by added 8-OHdG standards and prepared DNA samples for 10 min at room temperature. Then each well was added to 1:500 diluted anti-8-OHdG antibody and incubated for 1 h at room temperature on an orbital shaker. After washing 3 times 1X Wash Buffer supplied with the kit, the plate was incubated with diluted secondary antibody (1:1000) for 1 h at room temperature on an orbital shaker. At the end of the incubation, the washing step was repeated and then a color reaction was created by substrate solution. The reaction was stopped by adding a stop solution to each well of the plate. The absorbance was measured at 450 nm by subtracting

background absorbance at 640 nm. Results were calculated according to the standard curve. The detection range was 100 pg/ml-20 ng/ml.

3.10 Xenograft Tumor

3.10.1 Animals/ Xenograft mice

The experimental procedures were reviewed and approved by Acibadem Mehmet Ali Aydinlar University's local ethics committee for animal experiments (ACU-HADYEK 2015/30). Female 6–7 weeks athymic nude mice (Crl:NU(NCr)-Foxn1) were obtained from Charles River Laboratories (Germany). All used mice were kept under sterile conditions in isolated pathogen-free ventilation chambers under the ambient temperature of 20-22 °C and 45-50 % relative humidity. The animal rearing facility was maintained on a 12 h light-dark cycle. Mice were given free access to sterile food and water.

3.10.2 Tumor quantification

The cell suspension was prepared by trypsinization of confluent HCT116, HCT116 V1 or Lovo cells. The cell suspension was injected subcutaneously into the lower back region of the mice at the density of $5x10^6$ cells in a 100 µl 2:1 mixture of PBS: Matrigel (BD Biosciences). Mice were randomized into the control (DMSO 0.02 %) and CR (50 mg/kg) treatment groups. Mice were injected intraperitoneally every day for 3 weeks starting 7 days after cell injection. The tumor size was measured using calipers and (length x $width^2$) / 2 was used to calculate the tumor volume. The body weights of the mice were measured every day to determine systemic toxicity. Body weight change (BWC) was calculated by following the formula: [(body weight on the last day) - (body weight on day 0)] / (body weight on day 0) x 100. The concentration of CR used for this study is similar to other compounds that have been previously shown to be effective and well-tolerated in mice. After 3 weeks, sacrificing of the mice was performed using over-dose isoflurane.

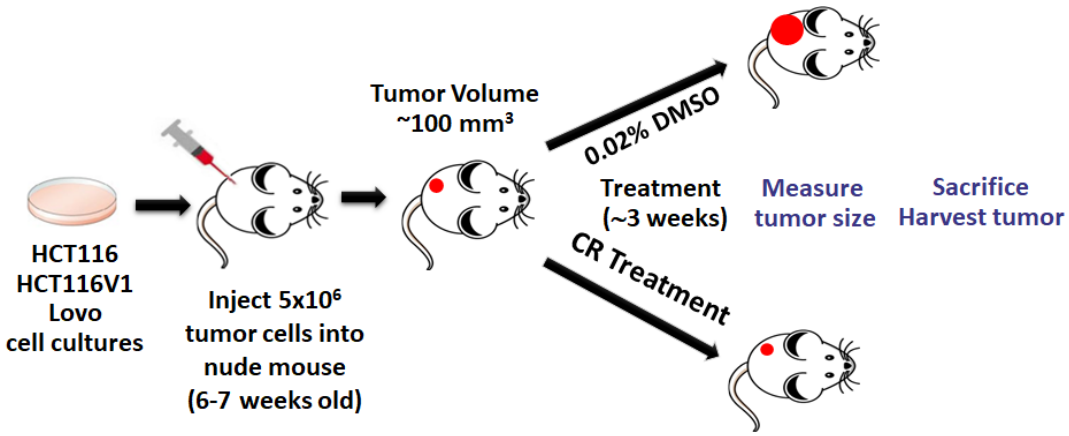

Figure 7. Evaluating the selective cytotoxicity of CR in xenograft mouse model.

3.11 Statistical Analysis

A two-tail student t-test (Prism 6, GraphPad Software) was performed and $p<0.05$ is considered significant.

4 RESULTS

4.1 Small Molecule Screening For Direct Binding To Pol γ

The Prestwick Chemical Library is a multi-format library that contains 1200 off-patent small molecules, which have been approved by the FDA, the European Medicines Agency, and other organizations and are ready for screening. We screened Prestwick Chemical Library molecules using SPR technology to find a Pol γ small molecule inhibitor that binds directly to the Pol γ holoenzyme. The Rmax of each compound was calculated by analyzing both Pol and RNA helix A. RNA helix A was used as a negative control protein to eliminating non-specific linkers. In the analysis result, 13 primary hits which bound Pol γ more than an arbitrary 3-fold higher than the negative control protein that demonstrated varying degrees of specific binding to Pol γ were identified(87).

We also used an in silico structural-based molecular docking approach to increase the screened pool, using the available crystal structure of Pol γ holoenzyme (PDB ID: 3IKM) and screening 8550 plant secondary metabolites from an in-house in silico library of drug-like compounds. One of the computationally predicted small molecules binds directly to Pol γ with high affinity, according to SPR kinetic analysis. This compound is CR (3,3'-[(1,1'-Biphenyl)-4',4'-diyl) bis(azo)] bis [4-amino-1-naphthalenesulfonic acid]; Zinc 03830554) found in the Zinc database. Biacore T100 software was used to calculate the association rate constant (ka or kON = 5.25E+4 1/Ms), dissociation rate constant (kd or koff = 0.029 1/s), and KD (0.5 0.05 μM) for CR (Fig 8)(87).

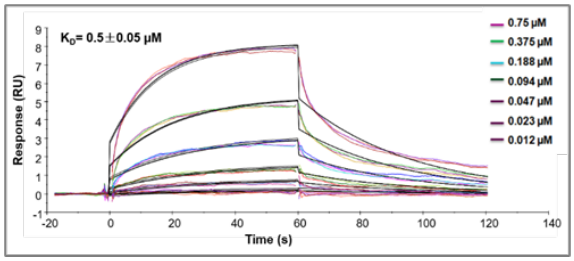

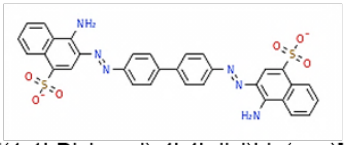

3,3'-[(1,1'-Biphenyl)-4',4'-diyl)bis(azo)]bis[4-amino-1-naphthalenesulfonic acid] (Congo red; Zinc 03830554)

Figure 8. Screening of Small Molecules for Direct Binding to Pol γ by SPR Technology.

4.2 Inhibitory Activity Of Small Molecules Directly Binding To Pol γ

We conducted *in vitro* activity assays with purified Pol γ protein to identify molecules that inhibit the biochemical activity of the Pol γ enzyme. We first tested the effects of the 10 Pol γ binder small molecules on Pol γ's strand displacement DNA synthesis activity using a 51mer DNA substrate with a 1-nt gap at position 26 (Fig 9A). CR, corilagin, and carbamazepine from the Zinc database (molecule number 1-3, respectively), phenolphthalein (molecule no. 4) from KEGG phytochemical compounds, and amethacin, indomethacin, amikacin hydrate 7 from Prestwick Chemistry Library (molecule number 5-7, respectively), and last three molecules, chenodiol, econazole nitrate, and ketoconazole from the Prestwick Chemical Library (molecule no 8-10, respectively), in the order in Figure 8B, it was tested on the strand displacement DNA synthesis activity of Pol γ at 20 µM. Each small molecule bound to the Pol γ protein had no significant effect on strand displacement DNA synthesis activity of Pol γ. This could be because the Pol γ protein's interaction with these small molecules did not affect its strand displacement activity. We found that CR inhibited the most, among the molecules tested with an estimated 98% (Fig 9B, lane 4, molecule no 1).

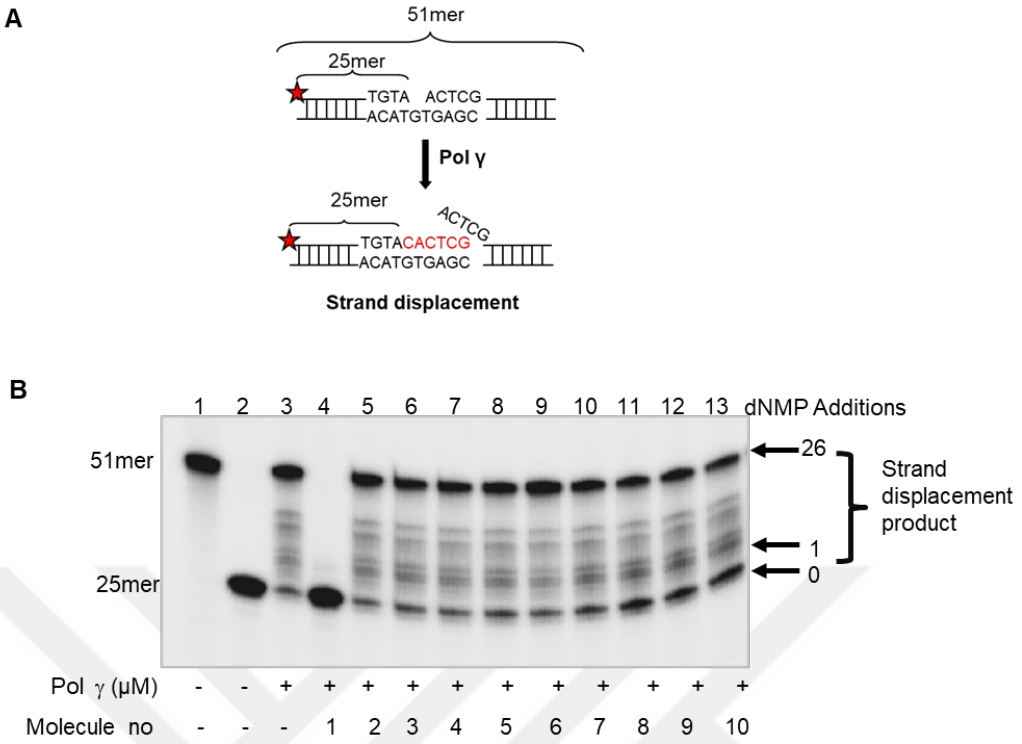

Figure 9. Screening the small molecules on the strand displacement DNA synthesis activity of Pol γ.

We performed additional functional assays with CR because it was the most effective inhibitor of strand displacement activity of Pol γ. We investigated the effects of increasing CR concentrations on the strand displacement and 1-nt incorporation activities of Pol γ (Fig 10A). Increasing concentration of CR (1.25, 2.5, 5, and 10 μM) (Fig 10B, lanes 4-7, respectively) significantly inhibited most of the substrates Pol γ (40 nM) strand displacement DNA synthesis in a concentration-dependent manner. The concentration of 5 μM CR inhibited Pol γ strand displacement DNA synthesis by nearly 94% (Fig 10B, lane 6). It demonstrated that CR did not change size when exposed to heat-inactivated Pol γ substrate, indicating that its inhibitory activity is not due to a potential impurity (Fig 10B, lane 8). We also tested how different concentrations of CR (1.25, 2.5, 5, and 10 μM) affected the 1-nt incorporation activity of Pol γ (Fig 10C). Again, 5 μM CR inhibited Pol's 1-nt incorporation activity by 95% and thus, we show that CR has a strong, concentration-dependent inhibitory effect on the Pol γ enzyme DNA synthesis activities.

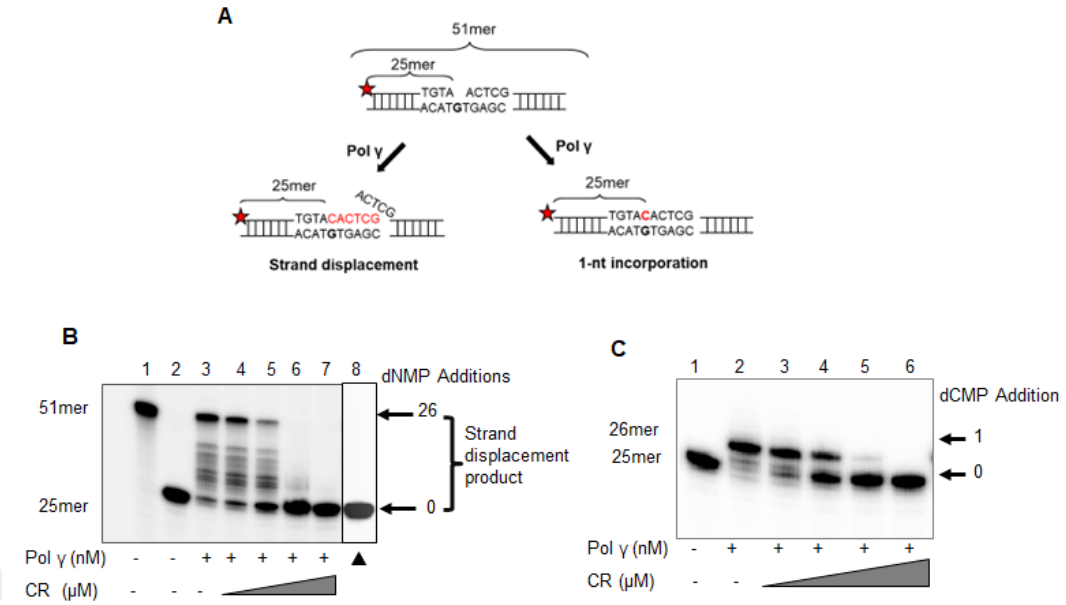

Figure 10. CR inhibits the DNA synthesis activity of purified Pol γ protein.

As another functional assay, we evaluated the effect of 1-nt incorporation DNA synthesis activity on both mitochondria and nucleus HCT116 extracts to assess the specificity to Pol γ of CR (Fig 11). The mitochondrial and nuclear markers complex IV (COX IV) and Lamin A/C were used to check for the absence of contamination in the samples (Fig 11A). The absence of nuclear contamination in mitochondrial extracts and mitochondrial contamination in nuclear extracts was confirmed by Western blot analysis. CR inhibited 1-nt DNA synthesis activity in mitochondrial extracts by about 2-fold, but it did not inhibit in nuclear extracts (Fig 11B). As a result of this assay, we demonstrated that CR is specific to mitochondrial DNA Pol γ.

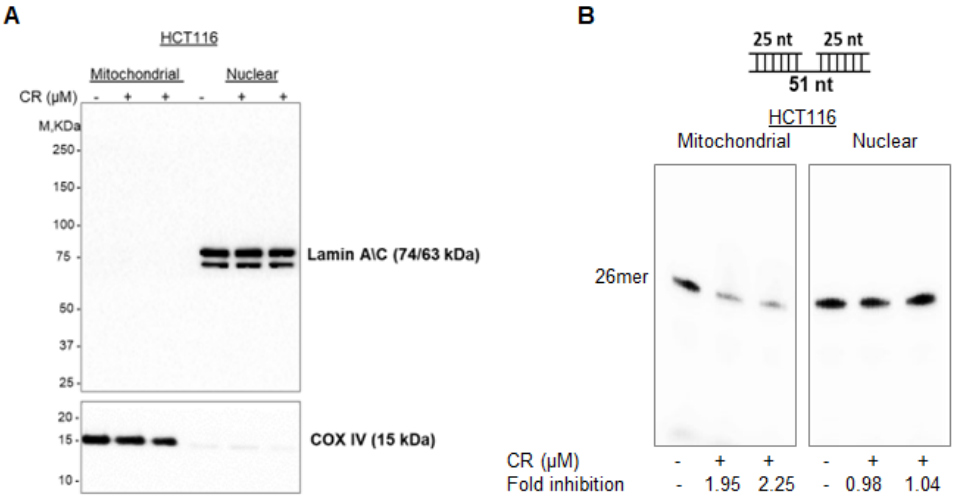

Figure 11. CR's selectivity was verified for mitochondrial Pol γ. (A) Western blot analysis of mitochondrial and nuclear extracts isolated from HCT116 cells confirmed the absence of nuclear contamination in the mitochondrial extracts and the absence of mitochondrial contamination in the nuclear extracts. (B) CR inhibits the DNA synthesis activity of mitochondrial cell extracts.

Lastly, to see if the inhibition of DNA synthesis by CR was specific for Pol γ, we examined the effect of CR on the bacterial E. coli DNA polymerase Klenow subunit. It needs 0.02 U Klenow polymerase for 95% of the substrate was converted to strand displacement products (Fig 12, lane 4). When assessed the effect of the strand displacement activity of the Klenow enzyme at the increasing concentrations of CR (1.25, 2.5, and 5 μM) (Fig 12, lane 3-5, respectively), only the highest concentration showed a 30% inhibition of Klenow DNA synthesis. As a result, even at this high concentration, CR was unable to completely inhibit the Klenow enzyme, as it did the Pol γ enzyme, which confirms the specificity of its inhibition.

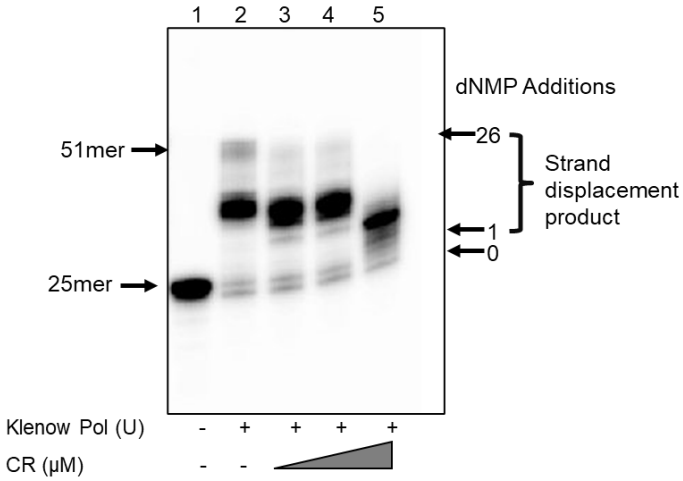

Figure 12. Klenow activity. Lane 1, substrate alone. Lane 2, Klenow (0.02 U/μl) alone, and lanes 3-5 are Klenow (0.02 U/μl) with increasing concentrations of CR (1.25, 2.5, and 5 μM).

4.3 CR Inhibits The Proliferation Of MLH1-Deficient Cancer Cells

We investigated the effect of CR, our top Pol γ inhibitor, on the cell proliferation of MLH1-deficient HCT116VA and MLH1-proficient HCT116V1 cells by using a real-time cell analysis xCELLigence instrument (Fig 14), because Pol γ inhibition selectively kills MLH1-deficient cancer cells(42). To that end firstly, we used western blot analysis to confirm that HCT116VA cells have MLH1 protein but HCT116V1 cells do not (Fig 13). HCT116, an MLH1-deficient cell line, was used as a control.

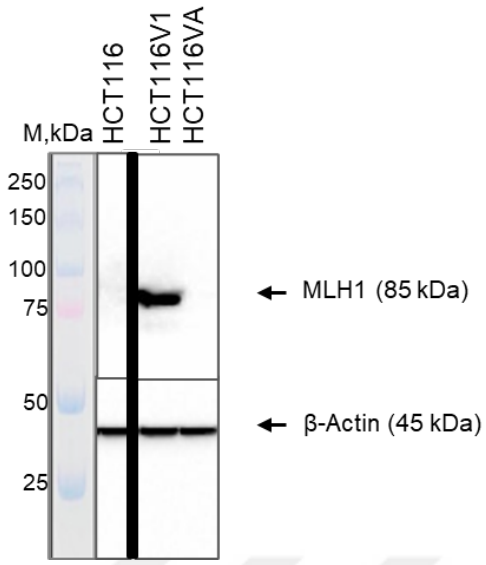

Figure 13. MLH1 levels of HCT116 cell lines were determined by Western blotting. β-actin is used as a loading control. M, Molecular marker-Precision plus protein dual-color standards from Bio-Rad.

We compared treatment with CR, our potential Pol γ inhibitor, at 20 μM using short-term real-time cell viability analyses on HCT116VA and HCT116V1 cells. 48 h after drug treatment, we calculated the IC_{50}value of CR on HCT116VA was 5.19 μM, whereas on HCT116 V1 this value was 1324 μM (Fig 14A-B). We then treated MLH1-proficient Lovo colon cancer and MCF7 breast cancer cell lines with increasing concentrations of CR to confirm CR function which targets MLH1-deficient cells. Even when the concentration was increased to 40 μM, we showed that CR did not affect the cell proliferation of MLH1-proficient cancer cell lines (Fig 14C and 14D). These experiments validated that CR may inhibit the proliferation of MLH1-deficient colon cancer cells selectively.

We also investigated the clonogenic long-term survival of HCT116VA and HCT116V1 cells after treatment with 5 μM CR based on their IC_{50} values at 48 h. We observed a 53 % reduction in the number of surviving HCT116VA colonies after long-term exposure to CR, while only a 25 % reduction in HCT116V1 colonies (Fig 14E). Thus, in both a short-term real-time cell viability assay and a long-term colony formation assay, MLH1-deficient HCT116VA cells were more sensitive to CR than MLH1-proficient HCT116V1 cells.

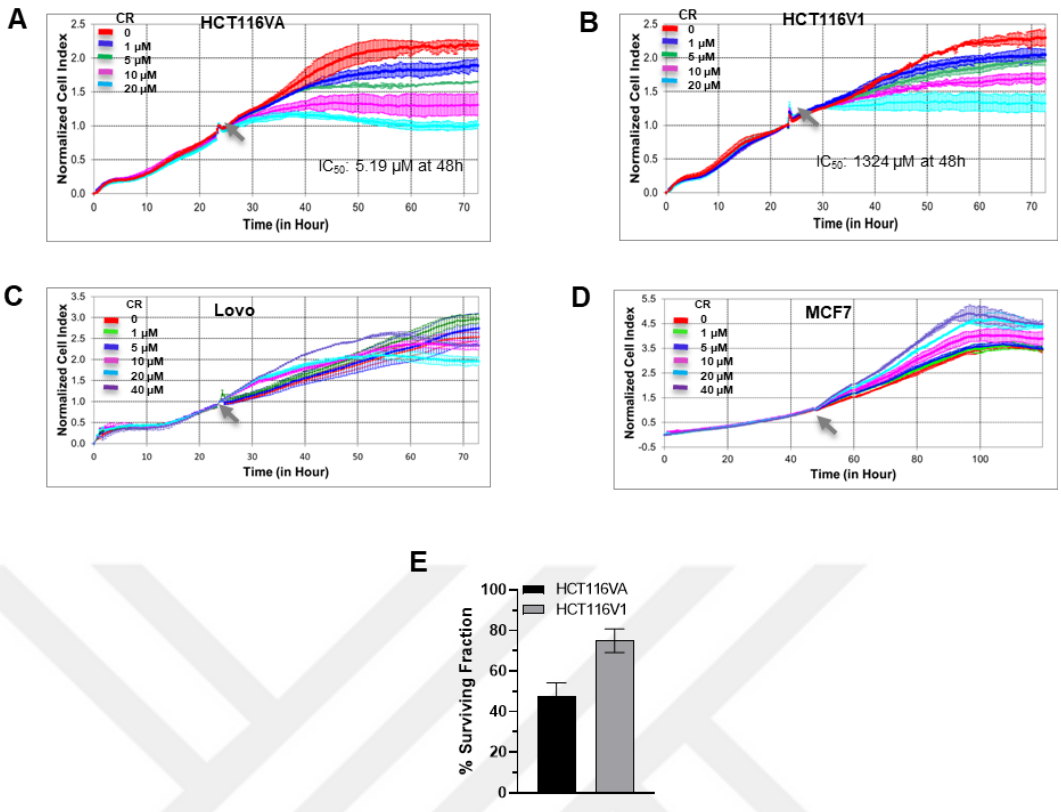

Figure 14. The effects of Pol γ inhibitor molecules on MLH1 deficient and proficient cancer cell proliferation.

4.4 Increased ROS Production In MLH1-Deficient Cell Lines Treated With CR

ROS causes structural changes or spontaneous DNA base mistakes that are repaired by BER(28), so we looked into the relationship between CR and ROS production in MLH1-deficient cells. To this end, we researched 8-OHdG levels of mt-DNA to measure the intracellular ROS production in MLH1-deficient (HCT116VA) and -proficient (HCT116V1) cell lines treated with vehicle control (DMSO) and CR (5 μM).

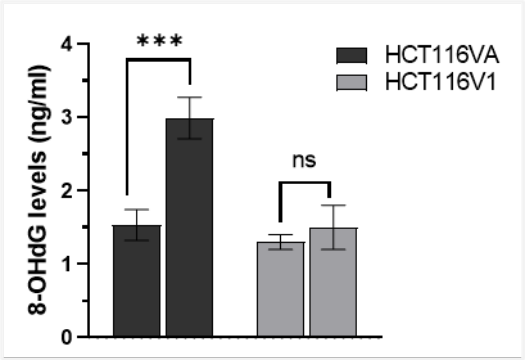

Figure 15. The quantification of 8-OHdG levels in HCT116 VA and HCT116 V1 cells upon treatment of CR ($p>0.05$).

We determined that CR increased 8-OHdG concentration in mtDNA of HCT116 VA cells by 1.95-fold (2.99±0.28 ng/ml). But our results indicated that there was no statistically significant difference in 8-OHdG levels in HCT116 V1 cells with upon addition of CR (Fig 15). The increase significantly in 8-OHdG levels in the HCT116VA compared to the HCT116 V1 upon addition of CR confirmed that CR, selectively in MLH1-deficient cells, causes oxidative mtDNA damage through an increase of ROS.

4.5 Suppressing Of HCT116 Xenograft Tumor Growth With CR Treatment

We were able to successfully test and validate a potential Pol γ inhibitor functional drug *in vivo* using athymic nude mouse xenografts. These experiments provided valuable information about drug toxicity and efficacy, which will be used to prioritize future *in vivo* testing.

We created HCT116, HCT116 V1, and Lovo xenograft tumor models in nude mice to validate our *in vitro* cellular findings that CR selectively inhibits the proliferation of MLH1-deficient HCT116 cells. When compared to vehicle-alone controls, CR at 25 and 50 mg/kg doses per day inhibited HCT116 xenograft tumor growth significantly. CR administration (50 mg/kg) resulted in a 67.33 percent decrease in tumor volume compared to the control group after 21 days (Fig 16A and 16B). The absence of significant body weight loss in comparison to control animals

demonstrated that both doses were well tolerated and nontoxic (Fig 16C). CR also does not affect tumor growth in HCT116 V1 (Fig 16D) or Lovo (Fig 16F and 16E) xenografts. These findings show that CR inhibits the growth of MLH1 deficient HCT116 xenograft tumors *in vivo* but not MLH1 proficient HCT116 V1 and Lovo xenograft tumors.

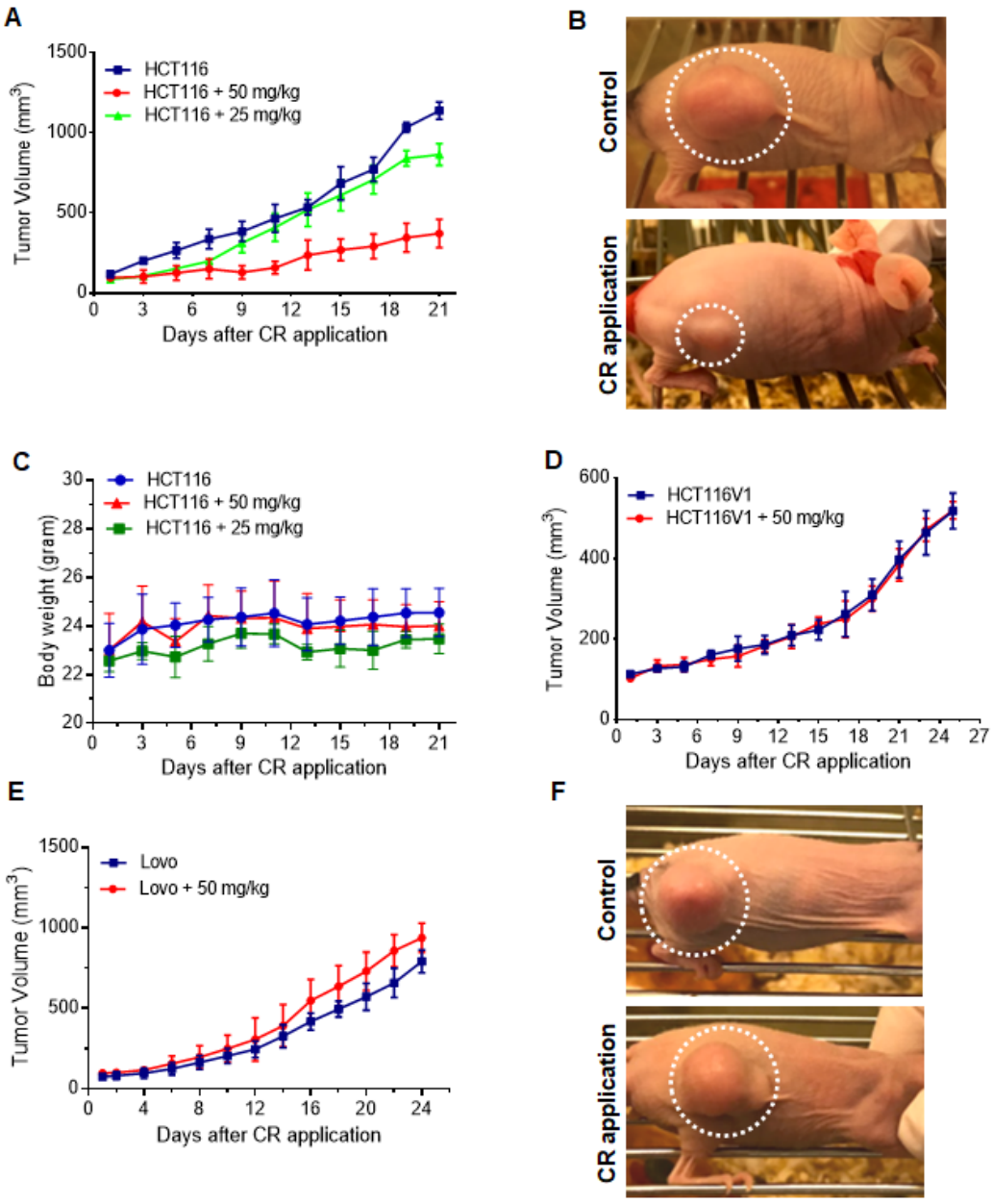

Figure 16. CR suppresses the growth of HCT116 xenograft tumors. (A) Growth curves of HCT116 xenograft tumors (n=6) treated with CR and 0.02 % DMSO (n=6). p <

0.01, 50 mg/kg compared with control group; p>0.05, 25 mg/kg compared with control group. (B) Tumor growth on HCT116 xenograft mice at end of 21 days. Control (0.02 % DMSO), and CR application (50 mg/kg). (C) The corresponding body weight changes during the treatment. p>0.05, compared with a control group. (D) Growth curves of HCT116 V1 xenograft tumors (n=3) treated with CR and 0.02% DMSO (n=3). p>0.05, compared with a control group. (E) Growth curves of Lovo xenograft tumors (n=5) treated with CR and 0.02 % DMSO (n=5). p>0.05, compared with a control group. (F) Tumor growth on Lovo xenograft mice at end of 21 days. Control (0.02 % DMSO), and CR application (50 mg/kg).

5 DISCUSSION

The ideal approach for successful cancer therapy is to selectively kill cancer cells while leaving normal cells alone. The BER mechanism, which plays an active role in the repair of DNA damage in cancer cells, is an important component in the prevention of cancer treatment, as it provides genomic stability by causing therapeutic resistance. HNPCC is caused by germline mutations in the MMR genes *MLH1* or *MSH2*, and in colorectal cancer cells with *MLH1* homozygous mutation(41), DNA damage is repaired by the mtBER pathway and cell viability is protected. Based on this synthetic lethal relationship between MLH1 and Pol γ, inhibition of the mtBER pathway could provide a promising approach for MLH1-deficient cancer therapy(42). The effect of Pol γ protein-specific inhibitors on mtDNA replication has been determined in a limited number of studies to date, but an inhibitor that selectively kills cancer cells has not been defined. We looked for new Pol γ inhibitor molecules that are selectively cytotoxic to MLH1-deficient cancer cells because known Pol γ inhibitors have not been used in the clinical treatment of MLH1-deficient cancers. The potent Pol γ inhibitor characterized in this study is CR, which binds to the Pol γ enzyme with high affinity, inhibits its activity specifically, and can slow the *in vivo* growth of MLH1-deficient cancer cells and tumor xenografts in a synthetic lethal manner.

The menadione an inhibitor of Pol γ, which is involved in mtDNA replication and repair, has been shown to inhibit Pol γ in cancer cells and increase superoxide levels compared to normal cells. Another study found that naphthoquinone, a menadione derivative, had a strong anti-proliferation effect on HCT116 cells(68). Furthermore, Martin et al. reported that mtDNA mutations were observed in patients treated with NRTI. This thesis study demonstrated that CR inhibits the DNA synthesis activity of Pol γ, thereby inhibiting the mtBER pathway. It was determined that CR, which was chosen from among the small molecules found to bind directly to the Pol γ protein, had a selective cytotoxic effect on the cell and caused mitochondrial damage. Our findings show that the new Pol γ inhibitor can selectively cause colon cancer cell death without damaging the healthy cell due to the synthetic lethal relationship between Pol γ and MLH1.

Recent cell viability-based small molecule screening studies have revealed that AS13 is selectively toxic to MLH1-deficient cancer cells and that menadione and cytosine-based nucleoside analogs such as cytarabine are selectively lethal to both MLH1- and MSH2-deficient cancer cells(42,83,88). The selective cytotoxicity of these compounds was associated with increased levels of cellular oxidative stress, most likely as a result of their ability to generate ROS, and as a consequence of cell cycle arrest, cell death was observed selectively in MLH1-deficient cancer cells(70,89). A recent study found that MLH1-deficient HCT116 cancer cells have a reduced antioxidant response, increased ROS, and are more vulnerable to DNA damage as a result of their disrupted mitochondrial metabolism(90). Here consistent with these findings, we demonstrated that CR was selectively cytotoxic to MMR-deficient cells as a potential therapeutic strategy. Our results suggest that treatment of MLH1-deficient HCT116 cells with CR increases ROS production and mtDNA 8-OHdG levels and not in MLH1-proficient HCT116 cells. The molecular basis of oxidative stress-induced selective cell death may differ between these cell lines. According to the findings, CR may cause mitochondrial dysfunction and death of cells by inhibiting Pol γ activity and oxidative mtDNA damage repair, and that incomplete repair of increased oxidative DNA damage in MLH1 deficient cells may induce selective cell death.

The azo class dyes have an exocyclic amino group that suffers oxidation or reduction processes in the body and further conversion to reactive electrophiles(65,67). For various periods, the azo class dyes used in textile, printing, chemical, food, and drug industries, including CR leads to toxic, mutagenic, and genotoxic effects due to ROS formation(66). Also, if this genotoxic effect is not reverted, it can induce a permanent mutation in the DNA. CR, on the other hand, has beneficial properties in that it inhibits amyloid oligomerization and fibril formation, as well as prevents protein aggregate accumulation and toxicity in neurodegenerative diseases such as Alzheimer's disease, and Huntington's disease, and spinocerebellar ataxia type 14(91,92). It was demonstrated that CR alleviates disease symptoms and increases life span in HD mice at a dose of 1 mg/30 g administered intraperitoneally every 48 h for 28 days(93). In our study, CR at 50 mg/kg, in other words, 1.5 mg/30 g, injected

intraperitoneally for 21 days showed the synthetic lethal antitumor effects without causing weight loss. It has also been shown that CR has virucidal effects by inhibiting RNA/DNA polymerase. Several cellular and animal studies have shown that the lethal dose of CR varies depending on the cell, tissue, and animal type, implying that using CR at the lowest possible dose would reduce its side effects. The lethal dose of CR in rats, for example, was estimated to be 190 mg/kg, and 400 mg/kg CR was lethal in pregnant rats(91).

CR seems to have minimal cytotoxicity to MLH1-proficient cells and leads to selectively killing MLH1-deficient cancer cells due to the synthetic lethal relationship between Pol γ and MLH1. Over the last few decades, nanoparticle based drug delivery systems have shown many advantages in cancer treatment, including precise targeting of tumor cells, reduction of drug side effects, decrease drug resistance, and also increase in the half-life of drugs(94). Transport of CR to mitochondria via nanocarrier systems is likely to increase its stability and therapeutic effect while decreasing off-target effects and toxicity. Therefore, further research into CR and its derivatives suggests that it could be a promising therapeutic agent for the treatment of MLH1-deficient cancers.

6 CONCLUSION

In this study, we showed that CR inhibits the DNA synthesis activities of Pol γ *in vitro* and *in vivo*. We also demonstrated that CR reduced the cell proliferation of MLH1 deficient HCT116 human colon cancer cells and suppressed HCT116 xenograft tumor growth whereas it did not affect the MLH1 proficient cell proliferation and xenograft tumor growth. CR increased the ROS production in MLH1-deficient cells compared to MLH1-proficient cells. This study suggests that the new Pol γ inhibitor, CR may be further evaluated for the MLH1-deficient cancers therapy.

7 REFERENCES

1. Babbar M, Basu S, Yang B, Croteau DL, Bohr VA. Mitophagy and DNA damage signaling in human aging. Mechanisms of Ageing and Development. 2020 Mar 1;186:111207.
2. Saki M, Prakash A. DNA damage related crosstalk between the nucleus and mitochondria. Free Radic Biol Med [Internet]. 2017 Jun 1 [cited 2022 Jun 2];107:216–27. Available from: https://pubmed.ncbi.nlm.nih.gov/27915046/
3. Lindahl T. Instability and decay of the primary structure of DNA. Nature [Internet]. 1993 [cited 2022 May 30];362(6422):709–15. Available from: https://pubmed.ncbi.nlm.nih.gov/8469282/
4. Jackson SP, Bartek J. The DNA-damage response in human biology and disease. Nature [Internet]. 2009 Oct 22 [cited 2022 May 30];461(7267):1071–8. Available from: https://pubmed.ncbi.nlm.nih.gov/19847258/
5. Jin B, Robertson KD. DNA methyltransferases, DNA damage repair, and cancer. Adv Exp Med Biol [Internet]. 2013 [cited 2022 May 30];754:3–29. Available from: https://pubmed.ncbi.nlm.nih.gov/22956494/
6. de Bont R, van Larebeke N. Endogenous DNA damage in humans: a review of quantitative data. Mutagenesis [Internet]. 2004 May [cited 2022 May 30];19(3):169–85. Available from: https://pubmed.ncbi.nlm.nih.gov/15123782/
7. Henle ES, Linn S. Formation, prevention, and repair of DNA damage by iron/hydrogen peroxide. J Biol Chem [Internet]. 1997 [cited 2022 May 30];272(31):19095–8. Available from: https://pubmed.ncbi.nlm.nih.gov/9235895/
8. Yonekura SI, Nakamura N, Yonei S, Zhang-Akiyama QM. Generation, biological consequences and repair mechanisms of cytosine deamination in DNA. J Radiat Res [Internet]. 2009 [cited 2022 May 30];50(1):19–26. Available from: https://pubmed.ncbi.nlm.nih.gov/18987436/
9. Demple B, Harrison L. Repair of oxidative damage to DNA: enzymology and biology. Annu Rev Biochem [Internet]. 1994 [cited 2022 May 30];63:915–48. Available from: https://pubmed.ncbi.nlm.nih.gov/7979257/
10. Montelone BA. DNA Repair and Mutagenesis. Second Edition. By Errol C Friedberg, Graham C Walker, Wolfram Siede, Richard D Wood, Roger A Schultz, and, Tom Ellenberger. Washington (DC): ASM Press. $179.95. xxix + 1118 p + 11 pl; ill.; index. ISBN: 1-55581-319-4. 2006. . https://doi.org/101086/509407 [Internet]. 2015 Jul 19 [cited 2022 May 30];81(3):273–273. Available from: https://www.journals.uchicago.edu/doi/abs/10.1086/509407
11. Cadet J, Davies KJA. Oxidative DNA damage & repair: An introduction. Free Radic Biol Med [Internet]. 2017 Jun 1 [cited 2022 May 30];107:2–12. Available from: https://pubmed.ncbi.nlm.nih.gov/28363603/

12. Tudek B, Bioteux S, Laval J. Biological properties of imidazole ring-opened N7-methylguanine in M13mp18 phage DNA. Nucleic Acids Res [Internet]. 1992 Jun 25 [cited 2022 May 30];20(12):3079–84. Available from: https://pubmed.ncbi.nlm.nih.gov/1620605/
13. Maynard S, Fang EF, Scheibye-Knudsen M, Croteau DL, Bohr VA. DNA Damage, DNA Repair, Aging, and Neurodegeneration. Cold Spring Harbor Perspectives in Medicine [Internet]. 2015 Oct 1 [cited 2022 May 30];5(10):a025130. Available from: http://perspectivesinmedicine.cshlp.org/content/5/10/a025130.full
14. Wang JYJ. Focus: Death: Cell Death Response to DNA Damage. The Yale Journal of Biology and Medicine [Internet]. 2019 Dec 1 [cited 2022 May 30];92(4):771. Available from: /pmc/articles/PMC6913835/
15. Harper JW, Elledge SJ. The DNA damage response: ten years after. Mol Cell [Internet]. 2007 Dec 14 [cited 2022 May 30];28(5):739–45. Available from: https://pubmed.ncbi.nlm.nih.gov/18082599/
16. Hegde ML, Hazra TK, Mitra S. Early Steps in the DNA Base Excision/Single-Strand Interruption Repair Pathway in Mammalian Cells. Cell Res [Internet]. 2008 Jan [cited 2022 May 30];18(1):27. Available from: /pmc/articles/PMC2692221/
17. Wang JC. Cellular roles of DNA topoisomerases: a molecular perspective. Nat Rev Mol Cell Biol [Internet]. 2002 [cited 2022 May 30];3(6):430–40. Available from: https://pubmed.ncbi.nlm.nih.gov/12042765/
18. Zhou W, Doetsch PW. Effects of abasic sites and DNA single-strand breaks on prokaryotic RNA polymerases. Proc Natl Acad Sci U S A [Internet]. 1993 Jul 7 [cited 2022 May 30];90(14):6601. Available from: /pmc/articles/PMC46980/?report=abstract
19. Heeres JT, Hergenrother PJ. Poly(ADP-ribose) makes a date with death. Current Opinion in Chemical Biology. 2007 Dec 1;11(6):644–53.
20. D'Amours D, Desnoyers S, D'Silva I, Poirier GG. Poly(ADP-ribosyl)ation reactions in the regulation of nuclear functions. Biochemical Journal [Internet]. 1999 Sep 9 [cited 2022 May 30];342(Pt 2):249. Available from: /pmc/articles/PMC1220459/?report=abstract
21. Davidovic L, Vodenicharov M, Affar EB, Poirier GG. Importance of poly(ADP-ribose) glycohydrolase in the control of poly(ADP-ribose) metabolism. Exp Cell Res [Internet]. 2001 Aug 1 [cited 2022 May 30];268(1):7–13. Available from: https://pubmed.ncbi.nlm.nih.gov/11461113/
22. McKinnon PJ, Caldecott KW. DNA Strand Break Repair and Human Genetic Disease. http://dx.doi.org/101146/annurev.genom7080505115648 [Internet]. 2007 Sep 21 [cited 2022 May 30];8:37–55. Available from: https://www.annualreviews.org/doi/abs/10.1146/annurev.genom.7.080505.115648
23. Fromme JC, Verdine GL. Base Excision Repair. Advances in Protein Chemistry. 2004 Jan 1;69:1–41.

24. Krokan HE, Bjørås M. Base excision repair. Cold Spring Harb Perspect Biol [Internet]. 2013 Apr [cited 2022 May 30];5(4):1–22. Available from: https://pubmed.ncbi.nlm.nih.gov/23545420/
25. Liu P, Demple B. DNA repair in mammalian mitochondria: Much more than we thought? Environ Mol Mutagen [Internet]. 2010 Jun [cited 2022 May 30];51(5):417–26. Available from: https://pubmed.ncbi.nlm.nih.gov/20544882/
26. Lindahl T. DNA glycosylases, endonucleases for apurinic/apyrimidinic sites, and base excision-repair. Prog Nucleic Acid Res Mol Biol [Internet]. 1979 Jan 1 [cited 2022 May 30];22(C):135–92. Available from: https://pubmed.ncbi.nlm.nih.gov/392601/
27. Wiebauer K, Jiricny J. Mismatch-specific thymine DNA glycosylase and DNA polymerase beta mediate the correction of G.T mispairs in nuclear extracts from human cells. Proc Natl Acad Sci U S A [Internet]. 1990 [cited 2022 May 30];87(15):5842. Available from: /pmc/articles/PMC54424/?report=abstract
28. Muftuoglu M, Mori MP, Souza-Pinto NC de. Formation and repair of oxidative damage in the mitochondrial DNA. Mitochondrion [Internet]. 2014 [cited 2022 Jun 3];17:164–81. Available from: https://pubmed.ncbi.nlm.nih.gov/24704805/
29. Izumi T, Mellon I. Base Excision Repair and Nucleotide Excision Repair. Genome Stability: From Virus to Human Application. 2016 Sep 21;275–302.
30. Demple B, Sung JS. Molecular and biological roles of Ape1 protein in mammalian base excision repair. DNA Repair (Amst) [Internet]. 2005 Dec 8 [cited 2022 May 30];4(12):1442–9. Available from: https://pubmed.ncbi.nlm.nih.gov/16199212/
31. Klungland A, Lindahl T. Second pathway for completion of human DNA base excision-repair: reconstitution with purified proteins and requirement for DNase IV (FEN1). EMBO J [Internet]. 1997 Jun 2 [cited 2022 May 31];16(11):3341–8. Available from: https://pubmed.ncbi.nlm.nih.gov/9214649/
32. Braithwaite EK, Prasad R, Shock DD, Hou EW, Beard WA, Wilson SH. DNA polymerase lambda mediates a back-up base excision repair activity in extracts of mouse embryonic fibroblasts. J Biol Chem [Internet]. 2005 May 6 [cited 2022 May 30];280(18):18469–75. Available from: https://pubmed.ncbi.nlm.nih.gov/15749700/
33. Kazak L, Reyes A, Holt IJ. Minimizing the damage: repair pathways keep mitochondrial DNA intact. Nature Reviews Molecular Cell Biology 2012 13:10 [Internet]. 2012 Sep 20 [cited 2022 May 30];13(10):659–71. Available from: https://www.nature.com/articles/nrm3439
34. Kajitani GS, Nascimento LL de S, Neves MR de C, Leandro G da S, Garcia CCM, Menck CFM. Transcription blockage by DNA damage in nucleotide excision repair-related neurological dysfunctions. Seminars in Cell & Developmental Biology [Internet]. 2020 Nov 21 [cited 2022 May 30];114:20–35. Available from: https://europepmc.org/article/med/33229217
35. Spivak G. Nucleotide excision repair in humans. DNA Repair (Amst) [Internet]. 2015 [cited 2022 May 30];36:13–8. Available from: https://pubmed.ncbi.nlm.nih.gov/26388429/

36. Volker M, Moné MJ, Karmakar P, van Hoffen A, Schul W, Vermeulen W, et al. Sequential assembly of the nucleotide excision repair factors in vivo. Mol Cell [Internet]. 2001 [cited 2022 May 30];8(1):213–24. Available from: https://pubmed.ncbi.nlm.nih.gov/11511374/
37. He D, Li T, Sheng M, Yang B. Exonuclease 1 (Exo1) Participates in Mammalian Non-Homologous End Joining and Contributes to Drug Resistance in Ovarian Cancer. Medical Science Monitor : International Medical Journal of Experimental and Clinical Research [Internet]. 2020 Mar 23 [cited 2022 May 30];26:e918751-1. Available from: /pmc/articles/PMC7092659/
38. Bowena N, Kolodnera RD. Reconstitution of Saccharomyces cerevisiae DNA polymerase e-dependent mismatch repair with purified proteins. Proc Natl Acad Sci U S A [Internet]. 2017 Apr 4 [cited 2022 May 30];114(14):3607–12. Available from: www.pnas.org/cgi/doi/10.1073/pnas.1701753114
39. Mei C, Lei L, Tan LM, Xu XJ, He BM, Luo C, et al. The role of single strand break repair pathways in cellular responses to camptothecin induced DNA damage. Biomedicine & pharmacotherapy = Biomedecine & pharmacotherapie [Internet]. 2020 May 1 [cited 2022 May 30];125. Available from: https://pubmed.ncbi.nlm.nih.gov/32036211/
40. Jacob S, Praz F. DNA mismatch repair defects: role in colorectal carcinogenesis. Biochimie [Internet]. 2002 [cited 2022 May 30];84(1):27–47. Available from: https://pubmed.ncbi.nlm.nih.gov/11900875/
41. Heinen CD. Mismatch repair defects and Lynch syndrome: the role of the basic scientist in the battle against cancer. DNA Repair (Amst) [Internet]. 2016 Feb 1 [cited 2022 May 30];38:127. Available from: /pmc/articles/PMC4740212/
42. Martin SA, McCabe N, Mullarkey M, Cummins R, Burgess DJ, Nakabeppu Y, et al. DNA Polymerases as Potential Therapeutic Targets for Cancers Deficient in the DNA Mismatch Repair Proteins MSH2 or MLH1. Cancer Cell [Internet]. 2010 Mar 3 [cited 2022 May 30];17(3–3):235. Available from: /pmc/articles/PMC2845806/
43. Braithwaite DK, Ito J. Compilation, alignment, and phylogenetic relationships of DNA polymerases. Nucleic Acids Res [Internet]. 1993 Feb 25 [cited 2022 May 31];21(4):787–802. Available from: https://pubmed.ncbi.nlm.nih.gov/8451181/
44. Hübscher U, Spadari S, Villani G, Maga G. DNA polymerases: Discovery, characterization and functions in cellular DNA transactions. DNA Polymerases: Discovery, Characterization and Functions in Cellular DNA Transactions. 2010 Jan 1;1–321.
45. Hoitsma NM, Whitaker AM, Schaich MA, Smith MR, Fairlamb MS, Freudenthal BD. Structure and function relationships in mammalian DNA polymerases. Cell Mol Life Sci [Internet]. 2020 Jan 1 [cited 2022 May 31];77(1):35–59. Available from: https://pubmed.ncbi.nlm.nih.gov/31722068/
46. Graziewicz MA, Longley MJ, Copeland WC. DNA polymerase gamma in mitochondrial DNA replication and repair. Chem Rev [Internet]. 2006 Feb [cited 2022 May 31];106(2):383–405. Available from: https://pubmed.ncbi.nlm.nih.gov/16464011/

47. Lim SE, Longley MJ, Copeland WC. The mitochondrial p55 accessory subunit of human DNA polymerase gamma enhances DNA binding, promotes processive DNA synthesis, and confers N-ethylmaleimide resistance. J Biol Chem [Internet]. 1999 Dec 31 [cited 2022 May 31];274(53):38197–203. Available from: https://pubmed.ncbi.nlm.nih.gov/10608893/
48. Uhler JP, Thörn C, Nicholls TJ, Matic S, Milenkovic D, Gustafsson CM, et al. MGME1 processes flaps into ligatable nicks in concert with DNA polymerase γ during mtDNA replication. Nucleic Acids Res [Internet]. 2016 Jul 8 [cited 2022 May 31];44(12):5861–71. Available from: https://pubmed.ncbi.nlm.nih.gov/27220468/
49. Yakubovskaya E, Chen Z, Carrodeguas JA, Kisker C, Bogenhagen DF. Functional human mitochondrial DNA polymerase gamma forms a heterotrimer. J Biol Chem [Internet]. 2006 Jan 6 [cited 2022 May 31];281(1):374–82. Available from: https://pubmed.ncbi.nlm.nih.gov/16263719/
50. Tropp BE. Molecular biology : genes to proteins. 2012;1097.
51. Ngo HB, Lovely GA, Phillips R, Chan DC. Distinct structural features of TFAM drive mitochondrial DNA packaging versus transcriptional activation. Nat Commun [Internet]. 2014 Jan 17 [cited 2022 May 31];5. Available from: https://pubmed.ncbi.nlm.nih.gov/24435062/
52. Kalifa L, Beutner G, Phadnis N, Sheu SS, Sia EA. Evidence for a role of FEN1 in maintaining mitochondrial DNA integrity. DNA Repair (Amst) [Internet]. 2009 Oct 2 [cited 2022 May 31];8(10):1242–9. Available from: https://pubmed.ncbi.nlm.nih.gov/19699691/
53. Copeland WC, Longley MJ. Mitochondrial genome maintenance in health and disease. DNA Repair (Amst) [Internet]. 2014 [cited 2022 May 31];19:190–8. Available from: https://pubmed.ncbi.nlm.nih.gov/24780559/
54. Zheng L, Zhou M, Guo Z, Lu H, Qian L, Dai H, et al. Human DNA2 is a mitochondrial nuclease/helicase for efficient processing of DNA replication and repair intermediates. Mol Cell [Internet]. 2008 Nov 11 [cited 2022 May 31];32(3):325. Available from: /pmc/articles/PMC2636562/
55. Young MJ, Copeland WC. Human mitochondrial DNA replication machinery and disease. Curr Opin Genet Dev [Internet]. 2016 Jun 1 [cited 2022 Jun 3];38:52. Available from: /pmc/articles/PMC5055853/
56. Sharma P, Sampath H. Mitochondrial DNA Integrity: Role in Health and Disease. Cells [Internet]. 2019 Jan 29 [cited 2022 Jun 7];8(2):100. Available from: /pmc/articles/PMC6406942/
57. Slupphaug G, Kavli B, Krokan HE. The interacting pathways for prevention and repair of oxidative DNA damage. Mutat Res [Internet]. 2003 Oct 29 [cited 2022 Jun 6];531(1–2):231–51. Available from: https://pubmed.ncbi.nlm.nih.gov/14637258/
58. Nilsen H, Otterlei M, Haug T, Solum K, Nagelhus TA, Skorpen F, et al. Nuclear and mitochondrial uracil-DNA glycosylases are generated by alternative splicing and transcription from different positions in the UNG gene. Nucleic Acids Research [Internet]. 1997 Feb 2 [cited 2022 Jun 6];25(4):750. Available from: /pmc/articles/PMC146498/?report=abstract

59. Chattopadhyay R, Wiederhold L, Szczesny B, Boldogh I, Hazra TK, Izumi T, et al. Identification and characterization of mitochondrial abasic (AP)-endonuclease in mammalian cells. Nucleic Acids Research [Internet]. 2006 [cited 2022 Jun 6];34(7):2067. Available from: /pmc/articles/PMC1440881/
60. Robertson AB, Klungland A, Rognes T, Leiros I. DNA repair in mammalian cells: Base excision repair: the long and short of it. Cell Mol Life Sci [Internet]. 2009 Mar [cited 2022 Jun 6];66(6):981–93. Available from: https://pubmed.ncbi.nlm.nih.gov/19153658/
61. Gredilla R. DNA Damage and Base Excision Repair in Mitochondria and Their Role in Aging. Journal of Aging Research [Internet]. 2011 [cited 2022 Jun 6];2011. Available from: /pmc/articles/PMC3018712/
62. Bohr VA. DNA damage and its processing. relation to human disease. J Inherit Metab Dis [Internet]. 2002 [cited 2022 Jun 6];25(3):215–22. Available from: https://pubmed.ncbi.nlm.nih.gov/12137230/
63. Koczor CA, Lewis W. Nucleoside reverse transcriptase inhibitor toxicity and mitochondrial DNA. Expert Opin Drug Metab Toxicol [Internet]. 2010 Dec [cited 2022 May 31];6(12):1493–504. Available from: https://pubmed.ncbi.nlm.nih.gov/20929279/
64. Scatena R. Mitochondria and drugs. Adv Exp Med Biol [Internet]. 2012 [cited 2022 May 31];942:329–46. Available from: https://pubmed.ncbi.nlm.nih.gov/22399430/
65. Biswas SJ, Khuda-Bukhsh AR. Cytotoxic and genotoxic effects of the azo-dye p-dimethylaminoazobenzene in mice: a time-course study. Mutat Res [Internet]. 2005 Nov 10 [cited 2022 May 30];587(1–2):1–8. Available from: https://pubmed.ncbi.nlm.nih.gov/16202644/
66. Chung KT, Cerniglia CE. Mutagenicity of azo dyes: structure-activity relationships. Mutat Res [Internet]. 1992 [cited 2022 May 30];277(3):201–20. Available from: https://pubmed.ncbi.nlm.nih.gov/1381050/
67. Chequer FMD, Lizier TM, de Felício R, Zanoni MVB, Debonsi HM, Lopes NP, et al. Analyses of the genotoxic and mutagenic potential of the products formed after the biotransformation of the azo dye Disperse Red 1. Toxicol In Vitro [Internet]. 2011 Dec [cited 2022 May 30];25(8):2054–63. Available from: https://pubmed.ncbi.nlm.nih.gov/21907275/
68. Sasaki R, Suzuki Y, Yonezawa Y, Ota Y, Okamoto Y, Demizu Y, et al. DNA polymerase gamma inhibition by vitamin K3 induces mitochondria-mediated cytotoxicity in human cancer cells. Cancer Sci [Internet]. 2008 May [cited 2022 May 31];99(5):1040–8. Available from: https://pubmed.ncbi.nlm.nih.gov/18312466/
69. Sharma RA, Dianov GL. Targeting base excision repair to improve cancer therapies. Mol Aspects Med [Internet]. 2007 Jun [cited 2022 May 31];28(3–4):345–74. Available from: https://pubmed.ncbi.nlm.nih.gov/17706275/
70. Song DSS, Leong SW, Ng KW, Abas F, Shaari K, Leong CO, et al. Novel 2-Benzoyl-6-(2,3-Dimethoxybenzylidene)-Cyclohexenol Confers Selectivity toward Human MLH1 Defective Cancer Cells through Synthetic Lethality. SLAS Discovery [Internet]. 2019 Jun 1 [cited 2022

May 30];24(5):548–62. Available from: http://slas-discovery.org/article/S2472555222067806/fulltext

71. Ashworth A. A synthetic lethal therapeutic approach: poly(ADP) ribose polymerase inhibitors for the treatment of cancers deficient in DNA double-strand break repair. J Clin Oncol [Internet]. 2008 [cited 2022 Jun 2];26(22):3785–90. Available from: https://pubmed.ncbi.nlm.nih.gov/18591545/
72. Guo G, Zhang F, Gao R, Delsite R, Feng Z, Powell SN. DNA repair and synthetic lethality. Int J Oral Sci [Internet]. 2011 Oct [cited 2022 Jun 2];3(4):176–9. Available from: https://pubmed.ncbi.nlm.nih.gov/22010575/
73. O'Neil NJ, Bailey ML, Hieter P. Synthetic lethality and cancer. Nat Rev Genet [Internet]. 2017 Oct 1 [cited 2022 Jun 2];18(10):613–23. Available from: https://pubmed.ncbi.nlm.nih.gov/28649135/
74. Klinakis A, Karagiannis D, Rampias T. Targeting DNA repair in cancer: current state and novel approaches. Cell Mol Life Sci [Internet]. 2020 Feb 1 [cited 2022 Jun 2];77(4):677–703. Available from: https://pubmed.ncbi.nlm.nih.gov/31612241/
75. Nijman SMB. Synthetic lethality: General principles, utility and detection using genetic screens in human cells. FEBS Letters. 2011 Jan 3;585(1):1–6.
76. Farmer H, McCabe H, Lord CJ, Tutt AHJ, Johnson DA, Richardson TB, et al. Targeting the DNA repair defect in BRCA mutant cells as a therapeutic strategy. Nature [Internet]. 2005 Apr 14 [cited 2022 Jun 2];434(7035):917–21. Available from: https://pubmed.ncbi.nlm.nih.gov/15829967/
77. Lord CJ, Ashworth A. PARP Inhibitors: The First Synthetic Lethal Targeted Therapy. Science [Internet]. 2017 Mar 3 [cited 2022 Jun 2];355(6330):1152. Available from: /pmc/articles/PMC6175050/
78. Glaab WE, Hill RB, Skopek TR. Suppression of spontaneous and hydrogen peroxide-induced mutagenesis by the antioxidant ascorbate in mismatch repair-deficient human colon cancer cells. Carcinogenesis [Internet]. 2001 Oct 1 [cited 2022 Jun 2];22(10):1709–13. Available from: https://academic.oup.com/carcin/article/22/10/1709/2733730
79. Colussi C, Parlanti E, Degan P, Aquilina G, Barnes D, Macpherson P, et al. The Mammalian Mismatch Repair Pathway Removes DNA 8-oxodGMP Incorporated from the Oxidized dNTP Pool. Current Biology. 2002 Jun 4;12(11):912–8.
80. Martin SA, Hewish M, Sims D, Lord CJ, Ashworth A. Parallel high-throughput RNA interference screens identify PINK1 as a potential therapeutic target for the treatment of DNA mismatch repair-deficient cancers. Cancer Res [Internet]. 2011 Mar 1 [cited 2022 Jun 2];71(5):1836–48. Available from: https://pubmed.ncbi.nlm.nih.gov/21242281/
81. Ashworth A, Lord CJ, Reis-Filho JS. Genetic interactions in cancer progression and treatment. Cell [Internet]. 2011 Apr 1 [cited 2022 Jun 2];145(1):30–8. Available from: https://pubmed.ncbi.nlm.nih.gov/21458666/

82. Bridge G, Rashid S, Martin SA. DNA Mismatch Repair and Oxidative DNA Damage: Implications for Cancer Biology and Treatment. Cancers (Basel) [Internet]. 2014 [cited 2022 Jun 2];6(3):1597. Available from: /pmc/articles/PMC4190558/

83. Martin SA, McCarthy A, Barber LJ, Burgess DJ, Parry S, Lord CJ, et al. Methotrexate induces oxidative DNA damage and is selectively lethal to tumour cells with defects in the DNA mismatch repair gene MSH2. EMBO Mol Med [Internet]. 2009 Sep [cited 2022 May 31];1(6–7):323–37. Available from: https://pubmed.ncbi.nlm.nih.gov/20049736/

84. Çelik H, Hong SH, Colón-López DD, Han J, Kont YS, Minas TZ, et al. Identification of Novel Ezrin Inhibitors Targeting Metastatic Osteosarcoma by Screening Open Access Malaria Box. Mol Cancer Ther [Internet]. 2015 Nov 1 [cited 2022 Jun 3];14(11):2497–507. Available from: https://pubmed.ncbi.nlm.nih.gov/26358752/

85. Lee YS, Kennedy WD, Yin YW. Structural insight into processive human mitochondrial DNA synthesis and disease-related polymerase mutations. Cell [Internet]. 2009 Oct 16 [cited 2022 Jun 7];139(2):312–24. Available from: https://pubmed.ncbi.nlm.nih.gov/19837034/

86. Somuncu B, Keskin S, Merve Antmen F, Saglican Y, Ekmekcioglu A, Ertuzun T, et al. non-muscle invasive bladder cancer tissues have increased base excision repair capacity. Scientific RepoRtS |. 123AD;10:16371.

87. Somuncu B, Ekmekcioglu A, Antmen FM, Ertuzun T, Deniz E, Keskin N, et al. Targeting mitochondrial DNA polymerase gamma for selective inhibition of MLH1 deficient colon cancer growth. Sobol RW, editor. PLoS One [Internet]. 2022 Jun 3 [cited 2022 Jun 6];17(6):e0268391. Available from: https://pubmed.ncbi.nlm.nih.gov/35657956/

88. Hewish M, Martin SA, Elliott R, Cunningham D, Lord CJ, Ashworth A. Cytosine-based nucleoside analogs are selectively lethal to DNA mismatch repair-deficient tumour cells by enhancing levels of intracellular oxidative stress. British Journal of Cancer 2013 108:4 [Internet]. 2013 Jan 29 [cited 2022 May 30];108(4):983–92. Available from: https://www.nature.com/articles/bjc20133

89. Hewish M, Martin SA, Elliott R, Cunningham D, Lord CJ, Ashworth A. Cytosine-based nucleoside analogs are selectively lethal to DNA mismatch repair-deficient tumour cells by enhancing levels of intracellular oxidative stress. British Journal of Cancer 2013 108:4 [Internet]. 2013 Jan 29 [cited 2022 May 30];108(4):983–92. Available from: https://www.nature.com/articles/bjc20133

90. Rashid S, Freitas MO, Cucchi D, Bridge G, Yao Z, Gay L, et al. MLH1 deficiency leads to deregulated mitochondrial metabolism. Cell Death Dis [Internet]. 2019 Nov 1 [cited 2022 May 30];10(11). Available from: https://pubmed.ncbi.nlm.nih.gov/31641109/

91. Frid P, Anisimov S v., Popovic N. Congo red and protein aggregation in neurodegenerative diseases. Brain Res Rev [Internet]. 2007 Jan [cited 2022 May 30];53(1):135–60. Available from: https://pubmed.ncbi.nlm.nih.gov/16959325/

92. Seki T, Takahashi H, Yamamoto K, Ogawa K, Onji T, Adachi N, et al. Congo Red, an Amyloid-Inhibiting Compound, Alleviates Various Types of Cellular Dysfunction Triggered by Mutant

Protein Kinase Cγ That Causes Spinocerebellar Ataxia Type 14 (SCA14) by Inhibiting Oligomerization and Aggregation. Journal of Pharmacological Sciences. 2010 Jan 1;114(2):206–16.

93. Sánchez I, Mahlke C, Yuan J. Pivotal role of oligomerization in expanded polyglutamine neurodegenerative disorders. Nature [Internet]. 2003 Jan 23 [cited 2022 May 30];421(6921):373–9. Available from: https://pubmed.ncbi.nlm.nih.gov/12540902/

94. Yao Y, Zhou Y, Liu L, Xu Y, Chen Q, Wang Y, et al. Nanoparticle-Based Drug Delivery in Cancer Therapy and Its Role in Overcoming Drug Resistance. Front Mol Biosci [Internet]. 2020 Aug 20 [cited 2022 May 30];7. Available from: https://pubmed.ncbi.nlm.nih.gov/32974385/

8 APPENDIX

ACU-HADYEK ETHICS COMMITTEE APPROVAL

Appendix 2

This page is available in the following languages:

Creative Commons License Deed

Attribution 4.0 International (CC BY 4.0)

This is a human-readable summary of (and not a substitute for) the license.

You are free to:

Share — copy and redistribute the material in any medium or format

Adapt — remix, transform, and build upon the material

for any purpose, even commercially.

The licensor cannot revoke these freedoms as long as you follow the license terms.

Under the following terms:

Attribution — You must give appropriate credit, provide a link to the license, and indicate if changes were made. You may do so in any reasonable manner, but not in any way that suggests the licensor endorses you or your use.

No additional restrictions — You may not apply legal terms or technological measures that legally restrict others from doing anything the license permits.

Notices:

You do not have to comply with the license for elements of the material in the public domain or where your use is permitted by an applicable exception or limitation.

No warranties are given. The license may not give you all of the permissions necessary for your intended use. For example, other rights such as publicity, privacy, or moral rights may limit how you use the material.

9 CURRICULUM VITAE